International Journal of Engineering Trends and Technology
ISSN: 2231-5381/ https://doi.org/10.14445/22315381/IJETT-V74I8P137

Volume 74 Issue 8, 549-570, August 2026

Review Article

Computational Strategies in Ballistic Puncture Penetration of UHMWP-E Polymers

Nyangani Mtimkulu[1], John Ikome[2], Grace Kanakana-Katumba[3]

[1]*Department of industrial, Operations Management & Mechanical Engineering, (IEOMME) Vaal University of Technology, South Africa.*

[1]*Corresponding Author : 20321821@edu.vut.ac.za*

Received: 03 December 2025 Revised: 10 June 2026 Accepted: 22 July 2026 Published: 29 August 2026

Abstract - *Engineering ballistic materials development, optimization and improvement are primarily backed by scientific, experimental and mathematical theories and findings. This has led to the development of numerical strategies that are widely considered to effectively yield cost-effective and rapid materials development, and optimization for continuous improvement of existing materials. These numerical strategies incorporate the structural model, computations and analysis of materials data and have been intensively being applied in metallic ballistic materials. However, in ballistic polymer materials such as Ultra-High Molecular Weight Polyethylene (UHMWP-E), the numerical strategies are still at a developing stage. This paper attempts to provide a comprehensive review of constitutive models and numerical simulation technique models applied in ballistic materials for guidance in obtaining improved results and future use of projectile penetration models in UHMWP-E polymers.*

Keywords - *Terminal ballistics, UHMWP-E polymers, Constitutive models, Numerical simulation, Modelling.*

1. Introduction

In the analysis of engineering design and optimization of the target material characteristics and properties in the ballistic environment, legacy knowledge and trial-and-error empiricism, and experimentation, scientific and mathematical principles application are acceptable as a means of material failure quantification [1]. Experimental investigations, together with numerical simulations and analytical/empirical modelling or combination of these approaches, are amongst the most popular and common means of analyses [2]. The analyses are vital in the approximation of engineering solutions; however, conducting them is often costly with very high error margins, while experimentation is sometimes not feasible owing to economic, spatial or practical limitations [2]. For this reasons, there are developed approaches to combine all these to a single effective solution using computational methods following a predefined computational process. The computation process includes conceptualizing a problem containing a complex physical reality to form a design model that can be translated and replicated into mathematical abstract terms. From a replica, a computational tool, model, algorithm and/or technique is discretized in such a way that they effectively use step-by-step computations in application approximations with the ability to analyze errors [3, 4]. There are numerous developed and implemented computational methods that currently available, and the onus lays with the user to select the appropriate and suitable one, depending mainly on the efficiency of the operation and prevention mechanisms. On the other hand, there are also factors such as estimation costs, ease of execution and accessibility of software package for computations in determining the most accurate and reliable computational strategy to perform for estimating ballistic failures [5, 6].

The accuracy of improvement requires reduction in computational errors and understanding of its contributing factors, leading to good convergence, repeatable and similar results obtained when similar input data is provided [7]. The pleasant reality, on the other hand, is that numerical models are one of the best suitable, rapid, timely, optimal and less costly investigation methods that are reliable, safe and rapid in modern-day ballistic material design and improvement investigations [8]. Also, the numerical models incorporate results obtained experimentally within the mathematical model and are seen to be helpful in improving the analysis results where numerical theories are not sufficient for computations, as well as in complex systems. Subsequently, Park, Yoo [5] also cogitates that numerical methods carry more advantage form experimentation due to the ability to extrapolate the information about the material and impact properties or geometries beyond the experiment range [4]. When comparing experimental and computational results with proper adjustment of the model parameters, Krishnan, Rajan [8] notes increased accuracy in reasonable times and commends their ability to help in finding innovative materials. Reliability of results is informed by the stableness of the methods, bearing in mind that it is entirely possible to have an accurate method that is efficiently implemented but unstable [9]. Barbour and Krahn [3] warns against thinking that computational approximations are for the enhancement of predictive capabilities, while they actually are for enhancing engineering judgement. Simply put, the computational models are primarily a journey of discovery of complex behavior of our physical world based on the process, not prediction. Alternatively, the progressions in numerical simulations are considered a threat to analytical models' development by authors such as Rosenberg and Dekel [4]. However, they warn us of how they are crucial for understanding the physics and the important parameters which influence the numerical processes such that the appropriate constitutive relations can be selected for computations. Most significantly, the computational method has to result in improved consistency, accuracy of computations, efficiency of computational times and stability of results.

In an armor environment, the reality is that the enemy constantly develops the projectile, penetrators or kinetic fragments material that can best destroy the target objects with improved resistance to failure. For this reason, the target material also has to be constantly developed as a mechanism of counteraction. The most important factor in target material improvement in ballistics is the material's high-speed projectile penetration resistance, impact energy dissipation and damage containment [10]. Furthermore, Voiculescu, Geanta [11] asserts that an optimized target has to have the capability to absorb and redistribute the projectile's impact energy in order to stop the penetrating projectile. To achieve these, the thickness of the target material is often increased, but this adds weight to the system. To attain effectiveness per unit mass, Lenihan, Ronan [12] recommends numerous layers of thinner plates offset from one another compared to a single thick plate, this however has the setback of increasing the thickness and greater geometric complexity to the target. Nonetheless, Jovicic, Zavaliangos [10] applauds the gradient design concept for weight optimization of the materials without a significant reduction of ballistic resistance. These approaches and recommendations are costly if one has to implement and adopt for application, for this reason the numerical approach has proven to be more cost-effective.

Numerical approaches are already in use in the ballistic environment, mainly on metallic and composite materials. The selection of a suitable approach depends on the constitutive relationships used in computations to attain best fit to ballistic penetration data [13]

whereas seen in the works of Riegel III and Davison [14], the empirical and analytical approach models from first principles and fully discretized numerical solutions can be further refined from effective flow stress to derive constitutive relationships. These constitutive relationships are further used in the analysis of material properties and characteristics by describing the material's behavior and relationship (physical basis) mathematically with its parameters to develop the constitutive methods for the target behavior under a terminal ballistic environment [6]. These are developed from first principles by definition of impact flow behavior observed as the interaction occurs in a manner that matches numerical reasoning to achieve the relationship between deformation and states of traction [15]. Again, the model, according to Cortis, Nalli [15], has to assist in assessing the structural integrity by identification of the elastic limits, ductility elasto-plastic behavior, and ultimate strength of the material under all ballistic operating conditions. Also, the best suitable model has to fully express and predict experimentally obtained information throughout the terminal ballistic stage and not only the end state [16]. Moreover, the model's success depends on the material's physical basis, flexibility and simplicity of the model and computational accuracy [17]. Finally, the numerical model boasts its cost-effectiveness, rapidness, accuracy and visualization, risk management capabilities, complex scenario application, efficient optimization, as well as appropriate prediction and insight predictions in terminal ballistic design environment [18, 19]. To minimize costs in a ballistic environment, there is an increasing demand for materials that have high strength-to-weight ratios, like Ultra-High Molecular Weight Polyethylene (UHMWP-E) materials [20]. One setback regarding UHMWP-E materials is that their ballistic properties and behaviors are often unidentified, and there is no existing database to enable the material improvement design process [21]. Also, in UHMWP-E materials, the use of numerical models is still at an infant stages. For this reason, this paper aims to identify most suitably defining and applicable numerical models that are already used in metals and composites with potential for success in ballistic UHMWP-E implementation.

2. Material Behavior under Ballistic Impact

The ballistic process can be summarized as the motion of a projectile object being projected at high velocities (interior ballistics); it flies through an atmosphere (usually air, water or solid medium) in an exterior ballistics environment; and interacts with the target material (terminal ballistics), causing damage to the target as a result of high-speed impact penetration [4, 22]. While this paper only focuses on terminal ballistic stage, where an impulsive projectile object strikes the target at high velocity, the high-velocity projectile strike induces fast-moving shock waves that prompt high pressures and temperatures in the projectile and in the target in very short times [4, 12, 23]. At high projectile velocities, the kinetic energy is converted to plastic work in the interface of the target and projectile [24]. This results in material reaching their thermal transition where melting and even vaporization occurs; high strain rates and large deformations; as well as mechanical changes leading to loss of strength, local fracture and even total shattering [4, 25, 26].

The intense shock waves often result in pressure during the impact that is considerably higher than the strength of the material, where the values of the principal stresses in the target are equal to each other [4]. Additionally, the state of the compressed solid under this sudden shock loading is irreversible, for this reason, the system is assumed to be in thermodynamic equilibrium. Furthermore, the materials are presumed to obey constitutive relationships, i.e. the Mass, Momentum and Energy conservation laws and behave as fluids [5]. These presumptions are not merely predictive, they are abstracted from known theories and are aimed at improving our judgment and understanding of the response of the system [27]. Since the physical and mechanical properties of the projectile and target are sensitive to high loading rates, high pressures and temperatures; the scenario is regarded as dynamic by nature [4]. The failure or fracture of the target can thus be defined according to equivalent strain rate, stress triaxiality and transition temperatures [28]. The generalized Hook law may be considered for higher strain ranges since the mechanical resistance is a function of the elastic strain tensor following a linear relation [29, 30].

The impulsive temperature changes during the impact often cause significant changes in material properties such as strength, toughness, shape and size due to thermal softening. Since the impact is envisioned to result in high deformation rates and deformations beyond elastic limit, with strain rates well beyond the quasi-static rate; a number of repetitive calculations are required from the computational model to define effects of properties such as strain rate hardening, strain hardening and thermal softening [4, 14]. The sudden changes in material leads to unstable flow in the material's microstructure and cause drastic changes to characteristic properties and integrity of the target material [31]. Since thermal effects at the impact region are vitally important, it is worth noting that relevant temperatures are different for various materials since their material properties and geometrical parameters differ [4, 32].

From observations relating to dynamic impact, the material behavior can be defined by transient state conditions; and as such, the steady-state conditions will not be real. Moreover, in cases of velocity range below velocities generally associated with guns, where the impacts may be either elastic or inelastic, penetration or permanent damage may not occur are not part of the scope of this work [33].

One of the focus areas in minimizing the damage from the projectile is on the reduction of projectile kinetic energy, which is achieved by redefinition of the target material's morphology aimed to improve its high-speed projectile strength resistance. The process to achieve a suitable target material often involves mending materials with different characteristics by surface treatment, impregnation and composite manufacturing. Suitability of the material depends on its properties and characteristics, its capability to eliminate the damage, and understanding of its failure criterion from a materials design engineer's perspective [34]. The suitable target material has to possess the hardness, impact resistance and high-temperature tolerances to ideally attenuate or eliminate projectile penetration capabilities [35, 36]. To achieve these, the target has to decelerate the projectile; break the projectile into fragments and decelerate the fragments; or deform the projectile to a less efficient shape and decelerate it and deform, erode or absorb the projectile's residual kinetic energy until it is low enough to not be able to penetrate the target [37, 38]. The target is known to have good attenuation capabilities due to their high yield stress, bulk and shear modulus; higher resistance to deformation and resistance to fracture at high stress levels. However, should these factors not be sufficient to cause attenuation, the thickness of the material can be increased, but the weight will unfortunately increase as well [10]. Lenihan, Ronan [12] sums up the target materials as energy disruptive or absorbing, whereby the disruptive induce projectile fragmentation to disperse its kinetic energy, and the absorbing transfers the kinetic energy of the projectile to heat.

2.1. Computational Modeling Techniques

To discover, simulate, predict and test scenarios on complex systems and scenarios incorporating mathematical and physical behavior of the material, computerized sciences incorporated in hydrocodes are used [18, 39]. Techniques include mathematical models, numerical models, machine learning and artificial intelligence, agent-based, statistical, data-driven and optimization algorithm models [40]. These techniques provide structured cost savings, time optimization and maximal resource usage benefits with reduced ethical non-compliances compared to actual experimentation [41, 42].

The entire computational analysis process encompasses problem formulation, application of appropriate pre-defined constitutive models, numerical techniques and failure criterion characterization. Since it is impossible to simulate model failures in a single calculation, time-step and repeated iterative analysis, multiscale techniques such as the hierarchical method are used [43].

2.2. Data Acquisition

In order to link the physical, mathematical and digital expressions of a computational model, the computer signal is collected, processed and converted into an interpretable data containing boundary conditions, material behavior and characteristics; and mechanical properties.

The primary aim is to provide accurate, timely and reliable results for ballistic environment from inputs and boundary conditions with improved accuracy and predictability to replace subjective human observations with objective results even in complex scenarios.

2.3. Reproducibility and Predictability Requirements

As noted by Riegel III and Davison [14], it is common to consider and be impressed when a complex model matches the pre-defined data even when appropriate model methodology is applied wrongfully. In some cases, they note that the users toggle the variables until the numerical values correspond to the experimental. To ascertain the model's reproducibility, the authors of the models and their developments attained results and compared with those obtained experimentally. The comparison was in terms of the correlation coefficient, average root mean square error, normalized bias error and absolute average relative error, which are commonly employed to ascertain the model's predictability and reproducibility [44]. The correlation coefficient deduces a linear relationship between experimental and numerical results; according to Lin, Chen [45], they are not always efficient since the models are biased towards high or low values. Average absolute relative error and average root mean square error are calculated comparing the errors by each term, and normalized bias error estimates the mean bias in prediction, where a positive value indicates over-prediction and the negative indicates under prediction [46, 47].

3. Constitutive Models

The definition of the target material's deformation and failure behavior in a ballistic environment has, over the years, attracted the development of numerous constitutive models with formulations to simulate the anticipated outcomes while considering the material's isotropic and anisotropic behaviors. The behaviors of materials are simulated in different material classes in order to formulate the cost-effective and rapid development of other materials that are not yet tested in application. As such, to attain accurate simulation results from numerical models, the parameters and input data has to be accurate. Success in accuracy according to Abed and Voyiadjis [17] can be attributed to physical derivation of model basis used for material parameter definitions; the flexibility and simplicity of attaining material constants from a limited set of experimental data [17]; as well as the model's ability to capture static and/or dynamic behavior of the material in addition to being mathematically and computationally accurate [48, 49].

According to Mihajlović and Živković [27], there is no unique and distinct classification of computational model types yet, they recommend classifying models according to their behavioral properties relating to symbolic or abstract (in most cases numerical) and the real constitutive (physical, material) models. The analytical models that describe the behavior of materials in terminal ballistics are grouped into categories based on their derivation method and identification of defining constants: empirical (phenomenological) models, semi-empirical models, physical models, and artificial neural networks [44, 49-53]. Empirical models describe the flow behavior developed from empirical observations where the constants are identified by fitting the empirical equation to the experimental stress-strain data and material flow stresses obtained from mechanical tests [50, 54, 55]. Moreover, the behavior of the material is described by considering macroscopic quantities without considering its microstructure and also uses regression analysis and can be integrated into most hydrocodes easily [56-58]. Artificial neural networks are suitable for situations where nonlinearity between the flow stress and process variables that are mainly solved by regression analysis techniques, which does not require mathematical model postulation or identification of its parameters, leading to poor prediction capabilities of the model [44, 47]. Plus, the artificial neural network models uses artificial intelligence [51].

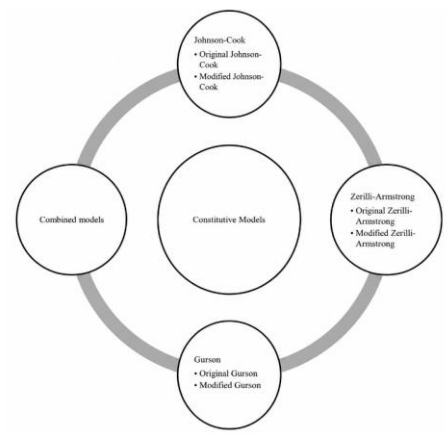

Fig. 1 Summary of models reviewed

This leads to simplified work and attaining what Epperson [9] perceives as a fusion of the study of the algorithms and their implementation methods with the study of the mathematical theory that supports them. Physical models are founded on the changes in the physical state of the material [54], and are derived using physical theories starting from the thermodynamics and kinetics of a dislocation slip [15, 50]; where the consideration to microstructure and physical aspects of material behavior is vital and they require more experimental data with a large number of material constants [31, 59, 60]. The semi-empirical models, on the other hand, are to some extent at the boundary of the empirical and physical models and are based on the fundamental physics, but constants-identification is similar to empirical models, with the equation fitted to the experimental data.

This work will attempt to explore the best suitable model for ballistic UHMWP-E target from Johnson-Cook, Zerilli-Armstrong and Gurson derived models as summarized in Figure 1 above.

3.1. Johnson-Cook Model

3.1.1. Original Johnson-Cook Model

Motivated by development of a computationally-efficient and empirical viscoplastic method based on von Mises flow stress criterion that could be calibrated with a relatively small number of laboratory tests without compromise to the output results and design cycle with increased insight understanding of loading conditions [14, 35, 50, 52, 61, 62]; Johnson [61] did the work in 1983 dealing with penetration mechanics, hardening and softening effect, strain rate and the effect of temperature with uncoupled multiplicative terms in ballistics; leading to a significant breakthrough amongst constitutive models [14]. This imperial model does not capture the physics of hardening, and can be used for maximum effective plastic strain failure, plus it is commonly used for isotropic ductile materials [63]. Additionally, this model is suitable where high-impact deformation rates are envisaged, resulting in a large number of iterative calculations and repetitive work due to effects of strain rate hardening or softening, strain hardening and thermal softening and can mimic the material behavior in severe ballistic conditions [5, 60, 64].

Material constants used in Jason-Cook models are typically determined from Quasi-static and dynamic tensile tests, Split Hopkinson Pressure Bar experiments, Taylor cylinder test, and high-temperature mechanical testing [14, 63]. Relatively high strain rates can be attained using split Hopkins pressure bar experiments, but Burley, Campbell [63] warns against possible uncertainties in data, similar to the Taylor cylinder test, due to the inability of the experiments to cover simultaneously high strain ranges and high strain rates. However, the Split Hopkins Pressure Bar is not accurate beyond necking in tensile specimens, and results tend to be complicated at large strains due to effects of adiabatic heating, where the net tensile stress becomes greater than the tensile flow stress resulting from the presence of hydrostatic tension. Also, at elevated temperatures, the material strength reduces as the material softens.

The model assumes isotropic material behavior and uses a power law, requiring relatively few material parameters across various high-strain-rate applications [35, 65, 66]. The constitutive equation for this model, as proposed by Johnson [61], includes the effects of plastic strain, strain rate, pressure, and temperature or adiabatic heating on the material strength [4, 67], and can be expressed as follows:

$$\sigma=(A+B\varepsilon^{n})\left(1-\left(\frac{T-T_{Room}}{T_{Melt}-T_{Room}}\right)^{m}\right)\left(1+Cln\left[\frac{\dot{\varepsilon}}{\dot{\varepsilon_o}}\right]\right) \quad (1)$$

where,

σ	Equivalent Flow Stress	B	Strain Hardening Coefficient
A	Yield Stress	C	Strain Rate Sensitivity Parameter
$\dot{\varepsilon}$	Equivalent Plastic Strain Rate	ε	Plastic Strain
$\dot{\varepsilon_o}$	Reference Strain Rate	n, m	Thermal softening and Strain Hardening Exponent
T_{Room}	Ambient Temperature	T_{Melt}	Melting Temperature of the Material

From Equation (1) above, the first term represents onset yield and hardening, the second term represents thermal effects, and third term relates to strain rates and dependence [15, 68]. Furthermore, this original model employs the Ludwik equation [69] that has the ability to define linear stress flow behavior of the material. Some authors have predicted the ineffectiveness of the equation when the stress flow behavior is non-linear and recommended the use of the Voce hardening concept [70].

The model captures mean stresses relatively well and also shows hardening that is often neglected in most computations. Also, it does not soften the yield surface with damage since there is no coupling of plasticity and failure models and is capable of reproducing strain to failure versus triaxiality data [71]. Furthermore, Burley, Campbell [63] attests that in the regime of subsonic impact velocities, the model results in a fairly realistic representation of reality, but it is not suitable for the quasi-static behavior of the materials. Additionally, the model has over the years gained popularity due to its lack of sophistication, simplicity, minor computational quantities, its intuitiveness that leads to constants approximated without loss of function, compatibility to a wide range of materials, and it is easy to understand and implement in finite element analysis codes at a rapid calculation speed despite its inability to analyze Lode angle effect [12, 52, 65, 71-73]. The model is considered simple to apply and computationally efficient since it has the ability to capture strain hardening, strain rate sensitivity, and thermal softening of the material in response to ballistic impacts, penetration, and explosive events [62, 74].

Model Behavior under Different Conditions

The original Johnson-Cook model as formulated in Equation (1) is not suitable for the estimation of the high-temperature flow behavior over the entire range of strain rates, temperatures and strains [49]. Thermal softening, strain rate hardening, and strain hardening are considered as three independent phenomena that can be isolated from each other in this model, but in reality, the coupled effect exists and has to be considered during the process of material deformation during the impact [75, 76].

The deformation process is categorized by elastic, plastic and steady stages, where in the elastic stage the linear correlation between flow stress and strain is observed, and in the plastic stage the flow stress does not behave proportionately to the strain. Whereas the dynamic recovery and recrystallization are main softening mechanisms experienced [77].

Effect on Strain Rate

At the initial stages of the experiment, the strain rate rises and can be characterized as thermal softening when the projectile impacts the target, resulting in dislocation motion; after this, the strain rate then eases [78]. At high strain rate, the strain hardening effect is strengthened, leading to high sensitivity at the affected region, and the dislocation motion crosses the barrier at short duration, which makes it difficult to overcome the barrier effects. The vibration amplitudes of material atoms are amplified by the heat, leading to dislocations motion domination [28].

At a constant strain rate, the flow stress decreases with temperature increase at the same strain due to thermal activation energy of the material and average kinetic energy, causing diffusion of atoms. The flow stress decreases with an increase in deformation temperature at constant strain rate, and strain rate increases with flow stress at constant temperature. Furthermore, high strain rates result in reduced dynamic recrystallization and energy accumulation, leading to rapid failure [47]. The shear stress decreases with an increase in temperature as a result of the shear stress required to initiate a slip. Also, dynamic recovery and recrystallization increase with temperature, causing a decrease in flow stress [77]. At the plastic deformation stage, the strain hardening dominates, and the dislocation propagates to increase the stress, and dynamic softening results from the pileup of dislocations at the hardening stage as the strain increases [77].

Effect on Temperature

The deformation temperature and strain rate affects the flow stress, since the deformation resistance increases with a decrease in temperature at constant strain rate and decreases with strain rate at constant temperature conditions. The deformation process results from work hardening (for material hardening) and dynamic recovery (material recovery and softening as a result of temperature rise, reducing flow stress) [45].

At high temperatures, the material endures strain-rate dependent superplastic deformation or wedge cracking. Additionally, the model describes thermal softening behavior nearly linearly, even though in reality it is saturated at higher temperatures, this leads to deviations in predictions [31].

The increase in flow stress to stress saturation as the strain increases translates to hardening on the stress-strain curve when the temperature is kept constant. Also, it decreases when the temperature is increased at a constant strain rate [77]. The strain-hardening rate is temperature dependent, as the temperature increases (leading to plastic deformation) the strain hardening decreases as the temperatures increase. With the increase in temperature, the stress decreases, and as the strain rate increases, so does the stress, and recrystallization gains can be seen. Whereas strain hardening occurs at all temperatures [79]. According to Iturbe, Giraud [80], the positive slope of the flow-stress curve indicates work hardening and the negative indicates softening, and these are a function of temperature. At constant temperature and strain, the flow stress increases with strain rate. The deformation at low temperature increases the dislocation density, and the strain hardening is dominant as seen from a microcosmic perspective. Softening dominates at higher temperatures [77]. The model shows that the temperature does not have an effect on the grain size and shape, but strain rate does refine the grain characteristics, and frailty is experienced at high temperature and high strain rate Wang, Guo [81].

The shortcoming of this model is that it overlooks the combined effect of the influential factors over the flow stress, reducing the accuracy of the constitutive equation; again, the adiabatic temperature rise during material deformation and a wide range of strain-rate sensitivity is not incorporated within the original model [82]. To overcome the limitations arising in the analysis, various modifications were made on the model's parameters (strain rates and dependence, onset yield and hardening and thermal effects) and are summarized in the next section.

3.1.2. Modified Johnson-Cook Models

Modifications Affecting Onset Yield and Hardening

Hou, Liu [54] realized the increase in strain rate resulting in an increase in stress rate, but the strain did not change much, this was noted to be true at varying temperatures. This led to their conclusion that the material's dynamic behavior depicts that there is a coupling effect between the strain and temperature; this motivated them to modify the model to predict the flow behavior at elevated temperatures and a diverse range of elevated strain rates. They further noted no coupling effect of strain and strain rate.

Modifications Affecting Strain Rates and Dependence

Kang, Cho [83] analyzed the strain hardening term at a point where it equates to 1 and concluded that at this point the term is negligible, and also that there is no significant impact resulting from temperature on the strain rate and also the results deviate from experimental data and overestimate strain rates above one. These discoveries led to their modification, focusing on the strain rate term to predict the dynamic behavior at high strain rates, and employing the quadratic curve fitting for interpolation rather than linear interpolation at a point where the strain hardening term is less than one.

Couque, Boulanger [84] and Johnson, Holmquist [85] on unrelated works, modified the strain rate term in the original model to enable the correlation of a power constant with the strain rate, where the strain rate was used to also define the transition between thermally activated and viscous regimes.

While experimenting at different strain rates, Wang, Huang [86] realized an independently occurring thermal softening phenomenon; at initial stages, the increase in strain rate led to the increase in flow stress and thereafter decreased and later increased again. They then concluded that thermal softening is caused by strain rate resulting from dislocation pileup rather than thermal effects.

Tan, Zhan [81] realized that the flow behavior of their studied materials is influenced by strain hardening and strain rate hardening, where high strain rates resulted in strain progression, and so it affected the strain hardening effect. They developed a modification that enabled varying of strain rate hardening coefficients with strain rate and strain.

The original Johnson-Cook does not describe the strain rate sensitivity, and depicts unreal and exaggerated particle deformation morphologies at high strain rates. Chakrabarty and Song [87] realized that at high strain rates the material experiences an additional drag mechanism which obstructs the movement of dislocations, leading to the increase in flow stress in the material, while at low strain rates the thermal energy and applied stresses causes the dislocation motion to overcome the barriers due to thermal activation. This realization led to the modification that captures strain-rate sensitive behavior by incorporating the strain gradient plasticity in the prediction of stresses and the final particle deformed shape [87].

Modifications Affecting Thermal Effects

Meyers, Chen [88] modified the original model by replacing the softening term with a temperature rise-dependent exponential term.

Hou and Wang [46] analyzed the mechanical and deformation behavior of materials under ballistic conditions and concluded that they depend on strain rate and temperature. They scrutinized the adiabatic temperature rise that causes thermal softening within the material as a result of plastic deformation and classified the process as isothermal. Furthermore, they found out that when the current temperature is lower than the reference temperature, quasi-static experimentation is highly impractical, and the temperature term in the original model cannot be solved in real ranges in this situation. The observations motivated them to modify the model for expansion to accommodate the applicability of the model at temperatures higher or lower than reference temperatures.

Chen, Ren [56] realized that at the beginning of plastic deformation, the work hardening rate is at its highest, then it decreases the increase in strain rate, stabilizes at quasi-static conditions and decreases with the increase in plastic strain at dynamic conditions as a result of dynamic recovery. From this, they concluded that the loading strain rate affects the work hardening rate and microstructure of the material, and they modified the model to incorporate the coupling effects of work hardening and strain rate, where thermal softening and logarithmic strain rate was suggested for flow behavior characterization [56]. Zhang, Liu [89] noted the thermal softening resulting from temperature increase leads to an increase in ultimate strain; this led to a modification of the softening term to predict the flow behavior on a wide temperature range and high strain rates based on the dependence of the softening parameter on temperature. This mixed temperature and strain model is characterized by the coupling of strain rate and temperature effect to formulate a single term.

Modifications Affecting Onset Yield and Hardening, and Strain Rates and Dependence

Rule and Jones [90] recognized that ductile metals experience enormous increases in yield stress at high strain rates and enhanced the model's sensitivity at high strain rates by extending the maximum attainable yield strength of the material.

Liu, Ma [28] used a multiple regression equation to define the coupling effects of strain rate and strain to predict the flow behavior at high temperatures and high strain rates.

Modifications Affecting Thermal Effects, Onset, Yield, and Hardening

Lin, Chen [45] realized the complexity of material behavior during deformation characterized by simultaneous hardening and dynamic recovery, where the temperature rise causes reduced flow stress and material softening.

They developed a modified model that considers the yield and strain hardening phenomenon in the prediction of the flow stress, with coupled effects of the temperature and strain rate considered.

In the modification by Li, Wang [47], both strain-hardening and softening terms are modified on the original model for the prediction of the flow behavior at elevated temperatures and different strain rates, considering the coupled effects of temperature and strain rate on the flow behaviors.

Modifications Affecting Strain Rates and Dependence, and Thermal Effects

Wang, Guo [81] continued from the work done by Rule and Jones [90] after realizing that the original Johnson-Cook model does not predict strain rate dependence of flow stress; and introduced the modification to predict the flow behavior at high strain rates and different temperatures, accounting for the coupling effect of anomalous temperature and strain rate dependence on flow stress.

Qian, Peng [58] noted the increase in flow stress as a result of strain rate increase and its decrease with temperature increase and thermal activation energy, and modified the model high strain rates and high temperatures application.

Since the original model requires the room temperature be higher than the reference, its applicability in a wide range of temperatures is limited, including at those lower than the reference. Wang, Zeng [21] modified the temperature term of the model with coupling effects based on temperature, elastic modulus, the specific heat at constant pressure, and Poisson's ratio using a multi-objective approach [21]. The multi-objectiveness of this non-linear model allows for analysis and an advanced genetic algorithm method to achieve undetermined parameters.

Priest, Ghadbeigi [55] realized that the original Johnson-Cook model possesses inadequate capabilities in the prediction of hardening and softening, and they modified the strain rate sensitivity and thermal softening parameters that led to improved temperature predictions compared with experiments.

He, Jun [91] noted that the logarithmic function and power law function of the Johnson-Cook formulation render it unreliable and inaccurate for the prediction of strain rate and temperature sensitivities when the relationship between the two is linear in reality. This motivated their argument that adding a quadratic term to a logarithmic strain rate term can better describe the flow stress and strain rate. This motivated their modified model for the prediction of flow behavior during warm bending at different temperature and strain rate ranges, with the strain rate term similar to the work of Kang, Cho [83]. Also, He, Jun [91] modification revealed that the thermal softening exponent at different strains and temperatures varies.

Modifications Affecting Strain Rates and Dependence, Onset Yield and Hardening and Thermal Effects

As noted by a number of researchers, the Jason-Cook meaning is a simple and clear model, but the strain rate hardening term is assumed to only increase linearly with logarithmic strain rate and also that thermal softening is linear, while in reality it is saturated at high temperature. Again, when the temperature is below room temperature, the homologous temperature is observed and results in the impossible softening term definition. Shin and Kim [92] compared Ludwik [69] and Voce [70] hardening laws in the strain rate term of the model and concluded that Ludwik hardening law is limited when the strain hardening is saturated, whereas Voce hardening law is able to describe the saturation of strain hardening and also when the strain hardening continues to progress with strain [92]. Voce hardening term usage enable the modified model to describe the linear rise in flow stress as a result of logarithmic strain rate at high strain rates with better precision for the development of physical models. Maheshwari, Pathak [93] modified the model for flow definition during material's hot deformation.

Wang, Han [94] modified the model to predict the flow behavior through a large range of strain rates and temperatures, accounting for coupling effect between the strain, strain rate, and temperature using Voce hardening to describe the strain-hardening term.

Lin, Li [94] modified model to predict the flow behavior under hot deformation, considering the coupling effect of strain, strain rate, and temperature during deformation.

Lin, Li [96] presented a modification to predict the flow behavior under hot deformation considering the coupling effect of strain, strain rate, and forming temperature.

Realizing that the flow stress increased as the strain rate increased and decreased as the temperature increased; Song, Ning [97] modified the model to predict the flow behavior matrix composite under strain rate and temperature conditions higher that reference since these two have an effect on the flow stress of the specimens [28].

According to Shokry [98], the slow rate of dynamic recovery and recrystallization causes the flow stress to decrease at high temperatures and low strain rates in hot deformation. Also, when the rate of dynamic recrystallization is increased at high temperatures, the dislocations are eliminated. After noting the noise in the experimental data, the authors decided to use a Kalman filter to accurately define the model parameters and minimize the mean square error between measured stress and predicted stress. Their modification affects the strain rate, temperature and softening parameters and introduces the coupling effect on these factors that affect the dislocation processes at higher temperatures and intermediary strain rates [60].

Zhao, Sun [78] continued from the work done by Lin, Chen [45] and devised a sine wave function for the strain rate term similar to the works of Wang, Huang [86] to predict the dynamic flow behavior in the material that considers thermal softening and strain hardening. They modified the strain-hardening term by fitting stress with strain with three-order polynomial functions instead of two-order polynomials at reference conditions.

Iturbe, Giraud [80] notes the strain hardening as a strain-related increasing function diverging to infinity and does not consider strain-softening phenomena. They observed the material go through strain hardening as a result of dislocation density and pileup, followed by softening where stress decreased with decreasing strain as a result of dislocation mobility until a critical strain level. The modification that develops the works of Lurdos, Montheillet [99], was proposed.

He, Chen [77], did a modification to predict the flow behavior at elevated temperatures and different strain rates, and thus presenting the coupling effects of strain, temperature and strain rates. Also, the modification accounts for initial deformation, recrystallization, work hardening and dynamic recovery.

Niu, Cao [79] did a modification that considers strain softening for accurate prediction of the flow behavior of the material at elevated temperatures and different strain rates, where the strain-hardening rate is modified to be interconnected with strain, and the strain rate is interrelated to strain and strain rate.

Li, Gao [57] modified the model to calculate the stress-strain curves at widely different strain hardening, strain rate and temperature conditions.

Yu, Li [100] predicted the flow behavior under hot deformation by modifying the softening term to account for the coupling effect of the temperature and strain rate from the original model.

Since the mechanism and dynamics of deformation vary in each material, Yu, Li [100] observed a linear increase in flow stress at an elastic stage; after yielding at the deformation stage, it increases with strain; and a decreased slope at the elastic stage. In the dynamic stage, a decrease in flow stress with increase in temperature was observed. These observations resulted in a proposed modification that considers the coupling effect of temperature and strain rate.

Another modification for flow behavior predictions on different element-based materials at high temperatures and a wide range of strain rates was proposed. This modified model considers the coupling effect of strain and strain rate, also that of strain, strain rate and temperature. This model, afterward, accommodates a number of shortcomings [72] and improves on other famous modified models, such as the one by Lin, Chen [45], to accommodate this shortcoming. For this reason, it is generally used in adiabatic transient dynamic analyses [15, 75]. The constitutive relation of the model from Shokry, Gowid [101] is given by:

$$\sigma=\left(\sum_{i=0}^{3} A_i\varepsilon^i\right)\left[1+\left(\sum_{i=0}^{2}\sum_{j=0}^{2} C_{ij}\varepsilon^i\varepsilon^j\right)ln\left[\frac{\dot{\varepsilon}}{\dot{\varepsilon_o}}\right]\right]e^{\left[\left(\sum_{i=0}^{2}\sum_{j=0}^{2}\sum_{k=0}^{2} m_{ijk}\varepsilon^i\varepsilon^j\left(\frac{T\text{-}T_{Room}}{T_{Melt}\text{-}T_{Room}}\right)^k\right)\left(\frac{T\text{-}T_{Room}}{T_{Melt}\text{-}T_{Room}}\right)\right]} \quad (2)$$

where,

σ	Equivalent Flow Stress	B	Strain Hardening Coefficient
A	Yield Stress	C	Strain Rate Sensitivity Parameter
$\dot{\varepsilon}$	Equivalent Plastic Strain Rate	ε	Plastic Strain
$\dot{\varepsilon_o}$	Reference Strain Rate	n, m	Thermal softening and Strain Hardening Exponent
T_{Room}	Ambient Temperature	T_{Melt}	Melting Temperature of the Material

A limited amount of work has been noted with regards to the model's applicability to anisotropic materials, microstructurally complex systems, and multi-physics material environments. The accuracy of the model and failure predictions is seen to degrade outside the calibration range and damage parameters. Furthermore, the model is not intended to capture the breadth of complex hardening behaviors. Also, it does not cater for crystalline forms at the microstructural level that can be altered due to the mechanical and thermal effects of ballistic strike.

The Johnson-Cook model is a strain rate and temperature-dependent phenomenology based on the local accumulation of plastic strain. It is widely used to simulate the damage of ductile materials with the ability to predict the damage onset point, and it is incapable of analyzing the damage evolution [102].

Moreover, Uhlmann, Polte [68] confirms that the model has now been successfully developed for use in polymers. The model is compatible with LS-DYNA, ABAQUS, AUTODYN & EPIC Finite Element Analysis (FEA) packages, and it is indispensable for engineers and researchers modelling material response [68].

3.2. Zerilli-Armstrong Model

3.2.1. Original Zerilli-Armstrong Model

In 1987, Zerilli and Armstrong [103] developed a phonological [17], viscoplastic, semi-empirical model based on thermal activation [15, 52], slip dislocation mechanisms (density and dynamics) theory for applications where high strain rates and elevated temperatures are envisioned at the microstructural level of different crystalline forms [50, 52, 59, 64, 104]. The effects of strain hardening and softening, strain-rate hardening, and temperature are systematically formulated and incorporated into the model to define the material's inelastic behavior [17, 105].

The model expresses thermally activated local dislocation motion obstacles and the dislocation interactions using two different classes of metal crystal structures, Face-Centered Cubic (FCC) and Body-Centered Cubic (BCC), and treats them differently [15, 106]. Since the strain rate and temperature sensitivities are different for these two families of materials, the model is able to capture microstructural effects such as dislocation motion [104]. Subsequently, coupling exists in reality between strain, strain rate, and temperature. In this instance, the preferred option based on a physical consideration of heat-activated dislocation motion and the interaction of individual dislocations with each other is the Zerilli-Armstrong model [59].

Body-centered cubic structure can be expressed as follows:

$$\sigma^y = A_0 + A_1 e^{[-A_3 T + A_4 T ln(\frac{\dot{\varepsilon}}{\varepsilon_0})]} + A_5 \varepsilon^n + \frac{k}{\sqrt{l}} \quad (3)$$

where,

σ^y	Flow Stress	ε	Equivalent Strain
A_i & n	Model Parameters	$\dot{\varepsilon_o}$	Reference Strain Rate
$\dot{\varepsilon}$	Plastic Strain Rate	T	Absolute Temperature
k	Microstructural stress intensity	l	Average grain diameter

From the above expression (Equation (3)), the plastic hardening is barely influenced by both strain rate and temperature except at the initial yielding point of the stress-strain curves [17]. The yield stress obtained in this model is decomposed into a thermal, thermally activated and viscous drag components [15]. An additional physical phenomenon to replace plastic flow with deformation twinning at high strains with stronger dependence in plastic yield stress on temperature and strain rate is one of the characteristics of this model as expressed in Equation (3). A thermal twinning stress is associated work hardening of the material and was seen to yield the results that suggest exaggerated strength of the material [103]. Additionally, the hardening stress is autonomous to both temperature and strain rate effects.

Nonetheless, in problems yielding high strain rates, the dynamic yield stress important expression to characterize the material behavior [17].

Alternatively, for Face Centered Cubic Structure, the original equation is expressed as:

$$\sigma^y = A_0 + A_2 \varepsilon^{p^n} e^{[-A_3 T + A_4 T ln(\frac{\dot{\varepsilon}}{\varepsilon_0})]} + \frac{k}{\sqrt{l}} \quad (4)$$

where,

σ^y	Flow Stress	ε	Equivalent Strain
A_i & n	Model Parameters	$\dot{\varepsilon_o}$	Reference Strain Rate
$\dot{\varepsilon}$	Plastic Strain Rate	T	Absolute Temperature
k	Microstructural stress intensity	l	Average grain diameter

From this formulation in Equation (4) The strain hardening is dependent on both temperature and strain rate, and this can be interpreted as the resistance to dislocation motion by the mutual interaction of dislocations according to Mha, Tongne [59]. Thermal activation analysis behavior depends on strain, leading to the elucidation that the intersection of dislocations is the controlling mechanism, while the dislocation-mechanics-based relations offer the possibility of accurately predicting the strain, stress, strain rate, and temperature at a point with sufficient accuracy to improve the current status of fracture modelling [103]. However, the flow stress threshold is independent of temperature and strain rate, resulting in a constant flow stress that is equal to the initial stress. Again, the grain size is not accounted for in Zerilli-Armstrong models even when it is a known fact that it will have a significant on the strength and ductility of materials [103]. On the contrary, the coupling effect of temperature and strain rate pertains primarily to the yield stress leading to cutting of dislocation forests [15, 17, 50, 107].

3.2.2. Modified Zerilli-Armstrong Models

Zerilli-Armstrong model is good for quasi-static tests where experimental data is not necessarily tracked by the predicted flow stress value predicted constitutive equation, since the model is applied to analyze both classes of materials as it considers their micro-structure under different strain rates and temperatures [49]. On the contrary, the model does not consider the connection between deformation and temperature effects [51, 59]. Again, the model is not effective at elevated temperatures; for these reasons, the modifications were developed to improve the model's ability to provide a ballistic impact solution.

Samantaray's Modified Zerilli-Armstrong Model

Since the original model cannot cater for above 60% melting temperatures [65]; where material parameters lose their physical meaning in application due to the exponential stress-temperature assumption [17], the modification was proposed by Samantaray, Mandal [108] to circumvent this problem using linear functions. According to Shokry [51], thermal activation analysis depends on plastic strain, which is controlled and dominated by the emergence and evolution of a heterogeneous microstructure of dislocations and the intersections amongst dislocations [14, 62]. Additionally, the temperature increase within the material is proportional to plastic strain, with the assumption that plastic work is converted to heat and ultimately adiabatic deformation occurs [17]. This includes the consideration of thermal softening, strain rate hardening and isotropic hardening as well as the coupled effects of temperature, strain and strain rate on flow stress with the ability to accurately describe the elevated temperature flow behavior of the materials [109].

According to Abed and Voyiadjis [17], Wang [52], Niu, Zhao [107], the yield stress at varying temperatures and strain rates do not reflect the reality due to the complexity of the coupled effect. The modified Zerilli-Armstrong equation can be summed up as:

$$\sigma^{y}=(A_1+A_2)+e^{\left[\left(A_3+A_4{\varepsilon^{p}}^{n}\right)(T+T_0)+(A_5+A_6(T\text{-}T_0)ln\left(\frac{\dot{\varepsilon}}{\varepsilon_0}\right)\right]} \tag{5}$$

Also, Samantaray, Mandal [108] proposed the modification expressed as:

$$\sigma^{y}=(A_1+A_2{\varepsilon^{p}}^{n})e^{\left[\text{-}\left(A_3+A_4\varepsilon+A_5\varepsilon^2\right)(T+T_0)+(A_6+A_7(T\text{-}T_0)ln\left(\frac{\dot{\varepsilon}}{\varepsilon_0}\right)\right]} \tag{6}$$

Where,

σ^{y}	Flow Stress	ε^{p}	Plastic Strain
A_i & n	Model Parameters	$\dot{\varepsilon_o}$	Reference Strain Rate
$\dot{\varepsilon}$	Plastic Strain Rate	T	Absolute Temperature

This modified Zerilli-Armstrong model cannot describe the behavior of some materials over the ranges of strain, strain rate and temperature [110]. Additionally, some materials cannot be approximated by linear functions, leading to the failure to reproduce the experimental results as expected.

This has led to the development of a model that takes these into account and its coupled effects to predict the evolution of the high-temperature flow threshold with decent correlation to the experimental data and good generalization at both low and high strain rate applications [62, 107].

Mha's Modified Zerilli-Armstrong Model

This developed model by Mha, Tongne [59], based on the modified Zerilli-Armstrong model, can be expressed as:

$$\sigma^{y}(\varepsilon^{p},\dot{\varepsilon}^{p},T)=\left(\sum_{i=0}^{q}A_i{\varepsilon^{p}}^{i}\right)+e^{[\left(\sum_{j=0}^{r}B_j{\varepsilon^{p}}^{j}\right)(T\text{-}T_0)+\left[\sum_{k=0}^{s}\left(\sum_{i=0}^{t}C_k{\varepsilon^{p}}^{l}\right)(T\text{-}T_0)^{k}\right]ln\left(\frac{\dot{\varepsilon}^{p}}{\varepsilon_0^{p}}\right)]} \tag{7}$$

where,

σ^{y}	Flow Stress	ε^{p}	Plastic Strain
C_i & n	Model Parameters	$\dot{\varepsilon_o}$	Reference Strain Rate
$\dot{\varepsilon}$	Plastic Strain Rate	T	Absolute Temperature

3.3. Gurson Model

3.3.1. Original Gurson Model

In 1977, Gurson [111] developed a model based on the analysis of the void in a perfectly plastic material using a yield criterion encompassing both hydrostatic stress and von Mises equivalent stress for ductile porous materials with the ability to simulate interactions of void growth under axisymmetric stress state [25, 102, 112-117]. The Gurson model became the first developed constitutive law for engineering materials to consider the effects of yielding of hydrostatic stress apart from the already existent bulk dilatancy. It analyzed the yield function isolated dilatational, pressure-sensitive and elasto-plastic voids [118].

The model assumes that the material is isotropic with quasi-static and isothermal conditions; and the effect of heat resulting from plastic deformation is neglected [112]. Under quasi-static loading conditions, Song, Ning [97] considers plastic deformation as an isothermal process and high strain rate deformation as an adiabatic process since the heat produced in this process cannot radiate quickly or be redistributed timeously [78, 97]. The plastic constitutive theory where the model was derived, consists of a function of stress defining stress at plastic yielding; the flow rule defining the ratio of strain component from stress state at yield [111]. The von Mises criterion is used in the characterization of the incompressible yield and flow behavior of the matrix to allow the void volume change in kinematic boundary conditions [111]. The model describes void nucleation or breaking as irreversible and can only occur at a positive increment of hydrostatic stress, and once it destabilizes, it forms rapid bulk softening and failure. The original Gurson equation can be expressed as [29]:

$$\frac{\dot{f_v}}{f_v\dot{\varepsilon}_p}=\frac{\left(\frac{2}{3}(1\text{-}f_v)sinh\left(\frac{2}{3}\sigma_h\right)\right)}{\sqrt{1+f_v^2\text{-}2f_v cosh\left(\frac{3\sigma_h}{2\sigma_y}\right)}} \tag{8}$$

where,

$\frac{\dot{f_v}}{f_v\dot{\varepsilon}_p}$	Equivalent Stress	f_v	Effective void volume function
σ_y	Tensile flow Stress	σ_h	Hydrostatic Stress

Fragmentation in ductile materials is often led by localized plastic deformation or adiabatic shear bands, causing strain localization as a result of destabilized material [113]. Large plastic deformation leading to material deterioration due to a high level of energy dissipation before fracture is considered as ductile damage; from a macroscopic crack that starts as cavity nucleation, then the cavity grows and then the cavity coalescence [119]. In computations, crack propagation is viewed as the growth of a traction-free boundary in the computational domain associated with the evolving and changing of the interpolation field [115]. Plastic deformation increases in ballistic materials causes a rapid increase in inclusions influenced by the rapid increase in strain within the material; the quantities and distribution of inclusions play an important role in material failure [120]. Wider distributed inclusions result in a decrease in material strength and plasticity, and they affect the fracture behavior of the material, while the area with a high number of inclusions will be the zone of fracture, leading to accelerated damage [121].

Again, the ductile fracture mechanism that leads to void growth and coalescence is not influenced by the mean stress except when the damage is invoked. In cases where the mean stress is zero, the stress state is pure shear, and no localization or material failure occurs since the void volume fraction is the damage parameter of the model [75, 122].

3.3.2. Modified Gurson Models

Gurson-Tvergaard-Needleman model

In 1981, Tvergaard [123] introduced a physics-based computational modification that is known as the Gurson model, which allowed for performing detailed calculations on an elastic--plastic medium containing a doubly periodic array of circular cylindrical voids with the ability to define the rupture process and critical void volume fraction within the material [115, 117, 120]. Lesuer, Kay [124] observed that Johnson-Cook and Zerilli-Armstrong do not accurately predict the failure of ductile materials characterized by the nucleation and growth of voids. This led to a successful pressure-sensitive macroscopic yield surface which relates void growth to the evolution of microscopic and macroscopic quantities to account for the behavior of void-containing solids.

The model was developed with transformation potential based on Gurson's work, where Gurson [111] (1977); Tvergaard [123] (1981); Tvergaard and Needleman [125] (1984) developed the Gurson-Tvergaard-Needleman model [112, 121]. This is a physically grounded failure model suitable for modelling ballistic penetration and spall in porous materials; and thermodynamic irreversible ductile fracture failure via void nucleation, growth, and coalescence of micro-voids under stress triaxiality. Park and Lee [73] define triaxiality as the ratio of hydrostatic stress and von Mises equivalent stress) [24, 102, 115, 116]. This phenomenological model further explained the phenomenon of sharp polymerization of voids during material rupture [118, 120] with better experimental agreement; and the ability to consider plastic strain, work hardening and cavity evolution until void coalescence [24, 119, 126, 127]. The yield function and plastic potential in the Gurson-Tvergaard-Needlemen model can be expressed in the following manner:

$$\Phi=\left(\frac{\Sigma}{\sigma}\right)^2+2q_1 f\cosh\left(\frac{3q_2\Sigma_m}{2\sigma}\right)\text{-}1\text{-}(q_1 f)^2=0 \qquad (9)$$

where,

Σ	Equivalent Stress	f	Effective void volume function
σ	Tensile flow Stress	Σ_m	Hydrostatic Stress
q_i	Material Parameters		

The model's setbacks include that it is not suitable for viscoplastic materials, which display significant rate-dependence, not suitable for a void shearing mechanism and also, stochastically determined parameters of void size, shape, orientation and spacing are often unknown [118, 128].

Other Modified Gurson Models

Further developments that incorporate void-growth-damage resulting from deviatoric stresses in addition to the hydrostatic stress were reported in the works of Kubair, Ramesh [113], where the model with the ability to account for the effects of dynamic loading and inertia on void-growth was developed. This model is suitable for continuum damage under pure-shear loading with quasi-static loading scenario derivations and the ability to analyze micromechanics behavior for both quasi-static and dynamic loading regimes. Again, the model is able to account for void-growth under shear deformation on an array of spherical voids.

From the work in 1999 by Lee and Oung [129] and Liao, Lin [130] in 2014, the model that could be used for porous materials incorporating the tensile-compressive asymmetry behavior can be obtained as follows [117]:

$$\Phi^{ct}(\Sigma_{ij},f,\xi)=\left(\frac{\Sigma_{eq}}{\sigma}\right)^2+2q_1 f\cosh\left(\frac{3q_2\Sigma_m}{2\sigma}\right)+(1\text{-}f)\eta\Sigma_m\text{-}1\text{-}(q_1 f)^2=0 \qquad (10)$$

with

$$\eta=\begin{cases}3(\sigma^{-1}M_t\text{-}\sigma^{-1}M_c),\ \xi>0\\ 3(\sigma^{-1}A_t\text{-}\sigma^{-1}A_c),\ \xi<0\end{cases} \qquad (11)$$

where,

Σ_{eq}	Equivalent Stress	f	Effective void volume function
σ	Mean (Hydrostatic) Stress	q_i	Empirical Constants

Recent developments into the model improved on incorporating void shape effects such as void distortion and inter-void interaction, analysis of viscoplastic materials containing microvoids and inclusions of the shearing fracture mechanism [118].

The yield surface of the Guson-Tvergaard-Needleman model takes into account the effect of the hydrostatic stress and decreases with the increase of the void volume fraction, which reflects the material deterioration characteristic with the damage development in the deformation process [120].

The conventional plasticity yield surface is larger, with a higher strain to failure ratio and has the ability to account for the influence of void formation on yield and flow behavior of a ductile metal [122, 124]. According to [131], the Tvergaard and Needleman coalescence criterion yields the lower values of critical porosity.Nahshon and Hutchinson [122] did a modification that allowed for analysis of damage rate development in shear by modelling localization and fracture in shear-dominated stress states with low triaxiality due to void rotation and distortion. This model was further extended by Nahshon and Xue [132] to develop the corresponding numerical implementation method in a VUMAT user material interface in ABAQUS Explicit.

Xue [133] extended the Gurson model to incorporate the dependence of ductile fracture on the third stress invariant by proposing void shearing damage using a separate damage indicator and yielding directly from the damage indicator in shear [118].

Nielsen and Tvergaard [134] realized that damage contribution is overestimated when stress triaxiality is high, but the ductile fracture prediction is accurate, and later in their work, Nielsen and Tvergaard [135] devised the shear stress contribution depending on the level of stress triaxiality to be able to capture mixed-mode fracture behavior. One of the setbacks relating to simulation of Gurson models is mainly dependent on finite element discretization, however this problem is mitigated by introducing a regularization method. Another simulation-related challenge is with regards to volumetric locking arising from quasi-plastic incompressibility, since traditional finite elements do not account for the kinematic incompressibility relation and preservation of enough degrees of freedom simultaneously [119]. Again, due to high plastic deformation causing plastic flow at the heat-affected impact zone in ductile fracture, Gurson models do not consider the thermo-mechanical coupling effect [115].

They are unable to capture strain localization and ductile fracture for shear stress-dominated problems, and when there is zero or negative mean stress, the increase in damage is not captured if there is no continuous void nucleation. This leads to an assumption that no damage-induced softening will ensue under shear in materials with inherent strain hardening capacity, and the computation will miss the details relating to localization and material failure [115].

The Gurson Model was modified to include void shape dependences by Gologanu, Leblond [136] (1995), and Pardoen and Hutchinson [137] (2000), who improved on the work of Leblond, Perrin [138] (1995). However, these modifications are based on solutions for voids in axisymmetric stress states and do not address the damage-induced softening in shear-dominated deformations [75].

The Gurson models have been implemented into ABAQUS via a user-defined material subroutine (VUMAT) [75, 112, 126] and in LS-DYNA [120, 124, 127].

3.4. Combined Models

Due to the complexity of the coupled effect of temperature and strain rate leading to unrealistic results [57], a combined Johnson-Cook and Zerilli-Armstrong model was proposed and given by:

$$\sigma=(A_1+B_1\varepsilon+B_2\varepsilon^{n_1})\left[\left(C_1+C_2 ln\left[\frac{\dot{\varepsilon}}{\dot{\varepsilon_o}}\right]\right)+\left(C_3+C_4 ln\left[\frac{\dot{\varepsilon}}{\dot{\varepsilon_o}}\right]\right)\left(\frac{T\text{-}T_{Room}}{T_{Melt}\text{-}T_{Room}}\right)^{\left(m_1+m_2 ln\left[\frac{\dot{\varepsilon}}{\dot{\varepsilon_o}}\right]\right)}\right] \quad (12)$$

where

σ	Equivalent Flow Stress	B	Strain Hardening Coefficient
A_1	Yield Stress	C	Strain Rate Sensitivity Parameter
$\dot{\varepsilon}$	Equivalent Plastic Strain Rate	ε	Plastic Strain
$\dot{\varepsilon_o}$	Reference Strain Rate	n	Strain Hardening Exponent
T_{Room}	Ambient Temperature	T_{Melt}	Melting Temperature of the Material

This combined the Johnson-Cook and Zerilli-Armstrong model aims to combine factors affecting the strain hardening effects and the strain rate effects with thermal softening in an incorporated formulation. Wang, Chandrashekhara [62] commends the model for enhanced strain hardening effect and the coupled effect of temperature and strain rate. However, parametric limitations relating to the accurate representation of experimental reality was observed [59].

The Zerilli-Armstrong, its modified models, and the combined Johnson-Cook and Zerilli-Armstrong models are compatible in LS-DYNA, ABAQUS (VUMAT), FORTRAN (VUHARD) and AUTODYN computational codes [17, 50, 59, 62, 108]. In these codes, Zhou, Yang [106] assessments suggests that the equivalent plastic strain, plastic strain rate, and temperature at the material point are iterated to determine the effective stresses and phase transformation-related state variables in a particular time increment.

4. Discussions

Models featured in this publication are phenomenological (Johnson-Cook and Gurson) and physical (Zerilli-Armstrong) based models; these models gained popularity as computational strategies due to the simplicity, cost-effectiveness and rapid production of results amongst a number of advantages they possess. Phenomenological models are generally simple to implement with lesser requirement for experimentation with lesser computational variables [46, 139]. The Johnson-Cook model considers strain hardening and is recognized to best describe the dynamic mechanical properties of nonferrous materials [54]. The model does not take into account the strain, strain rate-dependent and thermal-mechanical coupling effects, where the total rate of deformation can be decomposed to elastic, plastic, and thermal parts [82]. Furthermore, the model tends to over-predict yield stresses and under-predict strains at room temperature [12]. However, Wang [52], Cai, Wang [65] noticed that good predictions are only at reference temperature as a result of yield and strain hardening if the coupled effects of the temperature and strain rate on the flow behaviors are not considered.

According to Riegel III and Davison [14], the Johnson-Cook model over-predicts the influence of strain rate and has the ability to provide same results as Zerilli-Armstrong models. According to Xu, Yuan [64], the original Johnson-Cook model have a large deviation with limited prediction capabilities, and it is difficult to characterize the results at elevated temperatures when compared to Zerilli-Armstrong model due to the nonlinear coupled effect of temperature and strain rate [50, 82]. Zerilli-Armstrong model considers the microstructural orientation and dislocation densities of the material, adiabatic shear bands and strain localization. The Zerilli-Armstrong model is incapable of predicting actual experimental results at varying temperatures and strain rates but exhibits more flexibility than the Johnson-Cook model on predicting material properties [62, 106], while both use a power law stress-strain relationship that shows continual hardening without approaching saturation stress at high strains [140].

Strain hardening is represented graphically by Johnson-Cook model, and it can also be shown on the physical model. Microscopically, the strain hardening process begins at a point where dislocations are only gliding at the lowest energy paths until they reach higher energy, where they multiply; these rapid dislocations then grow in different directions depending on the material's shear modulus and orientation. Dislocations of the lattice become saturated and appear with lower strains, increasing to infinite plastic strain where the plastic strain becomes infinite [29].

High temperatures due to ballistic impact strikes complicates the microstructural changes within the material, resulting in simultaneous strain hardening, dynamic recovery, static and dynamic recrystallization [141]. Yet again, the material's deformation rate at higher strain rates depends on phonon and electron drag on moving dislocations [124].

Both of the phenomenological and physical models discussed in this publication have been improved and have shown good comparative results with reference to their original models in terms of either the correlation coefficient, average root mean square error, normalized bias error or absolute average relative error [47]. Authors such as Sastranegara, Putra [142], Haksever, Güden [143], Kubit, Trzepieciński [144] used Johnson-Cook model in their works and found it to be comparative with experimental results, with very low percentage errors. There are, however, other techniques with similar objectives to models discussed earlier, such as machine learning used in ballistic process analysis, Von Rueden, Mayer [145]. Machine learning mainly supports the computation process by detecting simulation patterns.

Velmurugan and Jeyaseelan [146] found that artificial neural networks were better suitable for the analysis of complex and intricate models than constitutive models such as Johnson-Cook. On the other hand, authors like Krzywanski, Sosnowski [40] are of the opinion that if artificial intelligence and machine learning's effectiveness are combined, they can provide even higher quality data. The predictions from artificial networks and machine learning result in relatively high efficiency, accuracy, robustness and simplicity at much lesser computational time [147]; however, they often cannot articulate the physical relationships between input and output variables, leading to difficulties in interpretation and trustworthiness in practical applications. Nguyen, Choi [148] noted that the combined effect of these techniques works incredibly well in microstructural modeling since they are able to identify and learn from data complex patterns, material properties and responses, and morphological parameters of the material.

In ballistic material selection processes, there is now an ever-growing need for detailed, specific and specialized design and manufacture [149-151]. The trend on specialized materials has been continuously improving, motivated by the need for specific properties and characteristics such as modulus and density in materials, tenacity and impact resistance [152, 153]. Amongst these materials, UHMWP-E has gained popularity in the ballistic environment and is competing favorably with most historically used metals.

According to Grujicic, Arakere [154], modern ballistic materials are now defined by their high-modulus/high-strength characteristics with outstanding impact resistance, examples include polymeric fibers such as aramids (Kevlar®, Technora® and Twaron®); (UHMWP-E) oriented polyethylene fibers (Spectra, Dyneema®); poly-benzobis-oxazole (Zylon®); and poly-pyridobisimi-dazole (M5. These characteristics in a material are determined according to the material's ballistic limit and the ballistic protection resistance.

Saruhan and Gunes [155] observed the development and application of advanced combat helmets made out of Kevlar® and noted that when compared to UHMWP-E, the projectile protection rate was at 37% and the density was 21.2% lower, putting UHMWP-E at an incredible position as a ballistic material. When tested in tension, UHMWP-E behaves like rate-independent linear elastic materials, and in transverse compression, they undergo large plastic deformation without a significant loss in their tensile load-carrying capacity. Again, the UHMWP-E materials are observed to have small diameters, high strength and a very low coefficient of friction which result in clamping failures during tensile testing [156]. According to [157], UHMWP-E in a terminal ballistics environment can be categorized as a ductile material in a ballistic environment; due to high entangled densities within the material as an interlocking mechanism, the material's morphology is considered crystalline [158]. This highly oriented and crystalline microstructure led to doubts from [159] as to whether the temperature degradation will follow Arrhenius behavior. For these reasons, the Jason-Cook, Zerilli-Armstrong, Gurson and its derived models are appropriate constitutive models for analysis of the material's behavior and responses in the ballistic environment.

5. Challenges and Future Work

While a number of modifications to different primary models discussed in this works exist to improve the reliability of results, there is still a huge potential for improvement, particularly in combined models. Already, the combination of Johnson-Cook and Zerilli-Armstrong models yielded good results, which may be a motivation to explore other model combinations, including using machine learning surrogates. Furthermore, different materials with their characteristics and properties behave differently when subjected to ballistic puncture; as a result, there cannot be a one-size-fits-all approach in determining the appropriate constitutive model to adopt for a specific material. This work anticipates to provide insight on the available model resources to aid in the decision to selection of the more appropriate for the particular scenario or material used.

6. Conclusions

This work included the review of phenomenological (Johnson-Cook and Gurson) and physical (Zerilli-Armstrong) based models that are used on other materials but were not yet introduced to analyze ballistic impacts in UHMWP-E materials with precision.

The precision of the numerical model in providing the numerical solution depends on how accurately the applied constitutive model describes the performance of the material and the implementation of the computational code; the inaccuracy leads to random or systematic errors in computations. Errors may emanate from faulty test conditions, physical characteristics of the model, position reference system calibration, defective model position and time measurements [33]. The understanding of mechanisms linked to the strain, strain rate and temperature effects are mandatory for constitutive modelling of the mechanical behavior in the ball of the material. According to Chocron and Anderson Jr [71], the physics incorporated in the model provides significant information with regards to reproducibility of failure patterns; von Mises-derived model does not reproduce slanted failure surfaces in compression and tensile tests due to a circular von Mises surface having no preferential direction for deformation or failure. Indeed, the resistance of all materials is always a response to the strain imposed by a loading. Elasticity as a reversible strain mechanism is present for all materials as a first step of strain, leading to the evolution of the internal thermodynamic variables being neglected.

Models discussed in this work have shown great potential for use in UHMWP-E materials, but with further exploration and more improvements may be recommended.

Conflicts of Interest

The authors declare that there is no conflict of interest regarding the publication of this paper.

References

[1] Mica Grujicic et al., "Application of the Materials-By-Design Approach to Armor-Grade Polymer-Matrix Composites for Enhancement of Ballistic-Penetration Resistance," *International Journal of Structural Integrity*, vol. 7, no. 1, pp. 142-174, 2016. [CrossRef] [Google Scholar] [Publisher Link]

[2] Andria Antoniou, Tore Børvik, and Martin Kristoffersen, "Evaluation of Automatic Versus Material Test-based Calibrations of Concrete Models for Ballistic Impact Simulations," *International Journal of Protective Structures*, vol. 15, no. 2, pp. 387-416, 2024. [CrossRef] [Google Scholar] [Publisher Link]

[3] S. Lee Barbour, and John Krahn, "Numerical Modelling–Prediction or Process," *Geotechnical News*, vol. 22, no. 4, pp. 44-52, 2004. [Google Scholar]

[4] Zvi Rosenberg, and Erez Dekel, *Terminal Ballistics*, 3rd ed., Springer Cham, 2012. [CrossRef] [Google Scholar] [Publisher Link]
[5] Myungsoo Park, Jeonghoon Yoo, and Dong-Teak Chung, "An Optimization of a Multi-Layered Plate Under Ballistic Impact," *International Journal of Solids and Structure*, vol. 42, no. 1, pp. 123-137, 2005. [CrossRef] [Google Scholar] [Publisher Link]
[6] Benno Stein, and Daniel Curatolo, "Selection of Numerical Methods in Specific Simulation Applications," *Tasks and Methods in Applied Artificial Intelligence: 11th International Conference on Industrial and Engineering Applications of Artificial Intelligence and Expert Systems, IEA-98-AIE*, Benicassim, Castellon, Spain, vol. 1416, pp. 918-927, 1998. [CrossRef] [Google Scholar] [Publisher Link]
[7] Eugene Isaacson, and Herbert Bishop, *Analysis of Numerical Methods*, Courier Corporation, 2012. [Google Scholar]
[8] K. Krishnan, S.D. Rajan, and A.D. Belegundu. "A General Optimization Methodology for Ballistic Panel Design," *Proceedings of the Engineering Optimization Conference*, 2008. [Google Scholar]
[9] James F. Epperson, *An Introduction to Numerical Methods and Analysis: Solutions Manual to Accompany*, John Wiley and Sons, 2014. [CrossRef] [Google Scholar] [Publisher Link]
[10] J. Jovicic, A. Zavaliangos, and F. Ko, "Modeling of the Ballistic Behavior of Gradient Design Composite Armors," *Composites Part A: Applied Science and Manufacturing*, vol. 31, no. 8, pp. 773-784, 2000. [CrossRef] [Google Scholar] [Publisher Link]
[11] I. Voiculescu et al., "Impact Behavior of the Ballistic Targets Package Composed of Dyneema Polymer and High Entropy Alloy Structures," *Archives of Metallurgy and Materials*, vol. 67, no. 2, pp. 569-576, 2022. [CrossRef] [Google Scholar]
[12] Donncha Lenihan et al., "A Review of the Integrity of Metallic Vehicle Armour to Projectile Attack," *Proceedings of the Institution of Mechanical Engineers, Part L: Journal of Materials: Design and Applications*, vol. 233, no. 1, pp. 73-94, 2018. [CrossRef] [Google Scholar] [Publisher Link]
[13] J.D. Clayton, "Methods for Analysis and Simulation of Ballistic Impact," *Recent Patents on Engineering*, vol. 11, no. 1, pp. 49-61, 2017. [CrossRef] [Google Scholar] [Publisher Link]
[14] John (Jack) P. Riegel III, and David Davison, "Consistent Constitutive Modeling of Metallic Target Penetration using Empirical, Analytical, and Numerical Penetration Models," *Defence Technology*, vol. 12, no. 2, pp. 201-213, 2016. [CrossRef] [Google Scholar] [Publisher Link]
[15] Gabriele Cortis et al., "Effects of Temperature and Strain Rate on the Ductility of an API X65 Grade Steel," *Applied Sciences*, vol. 12, no. 5, pp. 1-22, 2022. [CrossRef] [Google Scholar] [Publisher Link]
[16] D.E. Eakins, and N.N. Thadhani, "Instrumented Taylor Anvil-on-Rod Impact Tests for Validating Applicability of Standard Strength Models to Transient Deformation States," *Journal of Applied Physics*, vol. 100, no. 7, 2006. [CrossRef] [Google Scholar] [Publisher Link]
[17] F.H. Abed, and G.Z. Voyiadjis, "A Consistent Modified Zerilli-Armstrong Flow Stress Model for BCC and FCC Metals for Elevated Temperatures," *Mechanics Proceedings*, vol. 175, no. 1, pp. 1-18, 2005. [CrossRef] [Google Scholar] [Publisher Link]
[18] M. Elices et al., "The Cohesive Zone Model: Advantages, Limitations and Challenges," *Engineering Fracture Mechanics*, vol. 69, no. 2, pp. 137-163, 2002. [CrossRef] [Google Scholar] [Publisher Link]
[19] Krisn Pratap Meena et al., "Advantage of Numerical Analysis in Scientific Computation and its Applications," *Repository Antis Publisher*, 2023. [Google Scholar]
[20] Tuan-Long Chu, Cuong Ha-Minh, and Abdellatif Imad, "Analysis of Local and Global Localizations on the Failure Phenomenon of 3D Interlock Woven Fabrics under Ballistic Impact," *Composite Structures*, vol. 159, pp. 267-277, 2017. [CrossRef] [Google Scholar] [Publisher Link]
[21] Yuntian Wang et al., "Modified Johnson-Cook Constitutive Model of Metallic Materials under a Wide Range of Temperatures and Strain Rates," *Results in physics*, vol. 27, pp. 1-10, 2021. [CrossRef] [Google Scholar] [Publisher Link]
[22] Joe R. Gonzalez Jr, "Interior Ballistics Optimization," 1990. [Google Scholar]
[23] Tal Cohen, and David Durban, "Fundamental Solutions of Cavitation in Porous Solids: A Comparative Study," *Mechanics Proceedings*, vol. 224, no. 8, pp. 1695-1707, 2013. [CrossRef] [Google Scholar] [Publisher Link]
[24] Toshio Tsuta, Yajun Yin, and Takeshi Iwamoto, "Micro Damage Evolution Analysis of Target Impacted by Projectile," *JSME International Journal Series A Solid Mechanics and Material Engineering*, vol. 46, no. 2, pp. 109-118, 2003. [CrossRef] [Google Scholar] [Publisher Link]
[25] Fazle Rabbi Ahad, "*Modified Internal State Variable Models of Plasticity using Nonlocal Integrals in Damage and Gradients in Dislocation Density*," Mississippi State University, 2014. [Google Scholar] [Publisher Link]
[26] Anna Dmitruk et al., "Experimental and Numerical Study of Ballistic Resistance of Composites based on Sandwich Metallic Foams," *Applied Composite Materials*, vol. 28, no. 6, pp. 2021-2044, 2021. [CrossRef] [Google Scholar] [Publisher Link]
[27] Ivan Mihajlović, and Živan Živković, "Development of the Algorithm for Selection of Appropriate Numerical Modeling Approach," *Proceedings of FIKUSZ'14 Symposium for Young Researchers, Budapest, Hungary*, Obuda University, Keleti Faculty of Business and Management, Hungary, 2014. [Google Scholar] [Publisher Link]
[28] Xinyue Liu, Huihuan Ma, and Feng Fan, "Modified Johnson–Cook Model of SWRH82B Steel under Different Manufacturing and Cold-Drawing Conditions," *Journal of Constructional Steel Research*, vol. 186, pp. 1-16, 2021. [CrossRef] [Google Scholar] [Publisher Link]

[29] Charlesv Francart, "*Experimental and Numerical Study of the Mechanical Behavior of Metal/Polymer Multilayer Composite for Ballistic Protection*," University of Strasbourg, 2017. [Google Scholar] [Publisher Link]

[30] Srinivasan Gopalakrishnan, and Yapa Rajapakse, *Blast Mitigation Strategies in Marine Composite and Sandwich Structures*, 1st ed., Springer, Singapore, 2018. [CrossRef] [Google Scholar] [Publisher Link]

[31] P. Neelima, S.V.S. Narayana Murty, and P. Chakravarthy, "Comparison of Prediction Capabilities of Flow Stress by Various Constitutive Equation Models for Hot Deformation of Aluminum Matrix Composites," *Materials Performance and Characterization*, vol. 9, no. 2, pp. 237-261, 2020. [CrossRef] [Google Scholar] [Publisher Link]

[32] Xingsheng Sun, "Uncertainty Quantification of Material Properties in Ballistic Impact of Magnesium Alloys," *Materials*, vol. 15, no. 19, pp. 1-16, 2022. [CrossRef] [Google Scholar] [Publisher Link]

[33] Thomas N. Canning, Alvin Seiff, and Carlton S. Jame, *Ballistic-Range Technology*, 1970. [Google Scholar]

[34] Prabhani Ranaweera et al., "Ballistic Performance of Multi-Metal Systems," *International Journal of Protective Structures*, vol. 11, no. 3, pp. 379-410, 2020. [CrossRef] [Google Scholar] [Publisher Link]

[35] Bartosz Fikus, "Preliminary Numerical Estimation of Selected Terminal Ballistic Effects Produced by Explosion of Mortar Projectile," *Problems of Mechatronics. Armaments, Aviation, and Safety Engineering*, vol. 9, no. 1, pp. 49-60, 2018. [CrossRef] [Google Scholar] [Publisher Link]

[36] Jinhua Huang, Helen Durden, and Mostafiz Chowdhury, "Bio-Inspired Armor Protective Material Systems for Ballistic Shock Mitigation," *Materials and Design*, vol. 32, no. 7, pp. 3702-3710, 2011. [CrossRef] [Google Scholar] [Publisher Link]

[37] Bayode B. Adeyanju et al., "Materials and Manufacturing Process for the Ballistic Component: A Review," *International Journal of Novel Research in Engineering and Science*, vol. 11, no. 1, pp. 17-32, 2024. [CrossRef] [Google Scholar] [Publisher Link]

[38] Marvin E. Backman, *Terminal Ballistics*, 1976. [Google Scholar]

[39] Charles E. Anderson Jr, "An Overview of the Theory of Hydrocodes," *International Journal of Impact Engineering*, vol. 5, no. 1-4, pp. 33-59, 1987. [CrossRef] [Google Scholar] [Publisher Link]

[40] Jaroslaw Krzywanski et al., "Advanced Computational Methods for Modeling, Prediction and Optimization—A Review," *Materials*, vol. 17, no. 14, pp. 1-29, 2024. [CrossRef] [Google Scholar] [Publisher Link]

[41] Yale Chang, "Hydrocode Analysis at APL," *Johns Hopkins APL Technical Digest*, vol. 19, no. 1, pp. 72-81, 1998. [Google Scholar]

[42] S.H. Langer et al., *Performance Analysis and Optimization for Blast, a High Order Finite Element Hydro Code*, Lawrence Livermore National Laboratory (LLNL), Livermore, CA, 2015. [Google Scholar]

[43] Franck J. Vernerey et al., "The 3-D Computational Modeling of Shear-Dominated Ductile Failure in Steel," *JOM*, vol. 58, no. 12, pp. 45-51, 2006. [CrossRef] [Google Scholar] [Publisher Link]

[44] K.S. Prasad et al., "Prediction Capability of Constitutive Models for Inconel 718 Sheets Deformed at Various Elevated Temperatures and Strain Rates," *Materials Performance and Characterization*, vol. 8, no. 5, pp. 869-891, 2019. [CrossRef] [Google Scholar] [Publisher Link]

[45] Y.C. Lin, Xiao-Min Chen, and Ge Liu, "A Modified Johnson–Cook Model for Tensile Behaviors of Typical High-Strength Alloy Steel," *Materials Science and Engineering: A*, vol. 527, no. 26, pp. 6980-6986, 2010. [CrossRef] [Google Scholar] [Publisher Link]

[46] Qing Yu Hou, and Jing Tao Wang, "A Modified Johnson–Cook Constitutive Model for Mg–Gd–Y Alloy Extended to a Wide Range of Temperatures," *Computational Materials Science*, vol. 50, vo. 1, pp. 147-152, 2010. [CrossRef] [Google Scholar] [Publisher Link]

[47] Hong–Ying Li et al., "A Modified Johnson Cook Model for Elevated Temperature Flow Behavior of T24 Steel," *Materials Science and Engineering: A*, vol. 577, pp. 138-146, 2013. [CrossRef] [Google Scholar] [Publisher Link]

[48] M. Dolinski, and D. Rittel, "Experiments and Modeling of Ballistic Penetration using an Energy Failure Criterion," *Journal of the Mechanics and Physics of Solids*, vol. 83, pp. 1-18, 2015. [CrossRef] [Google Scholar] [Publisher Link]

[49] Bing Zhang et al., "A Comparative Study on Johnson–Cook, Modified Johnson–Cook, Modified Zerilli–Armstrong and Arrhenius-Type constitutive Models to Predict Hot Deformation Behavior of TA2," *High Temperature Materials and Processes*, vol. 38, no. 2019, pp. 699-714, 2019. [CrossRef] [Google Scholar] [Publisher Link]

[50] Murali Mohan Gurusamy, and Balkrishna C. Rao, "On the Performance of Modified Zerilli-Armstrong Constitutive Model in Simulating the Metal-Cutting Process," *Journal of Manufacturing Processes*, vol. 28, pp. 253-265, 2017. [CrossRef] [Google Scholar] [Publisher Link]

[51] Abdallah Shokry, "Modified Fields-Backofen and Zerilli-Armstrong Constitutive Models to Predict the Hot Deformation Behavior in Titanium-based Alloys," *Scientific Reports*, vol. 14, no. 1, pp. 1-19, 2024. [CrossRef] [Google Scholar] [Publisher Link]

[52] Xin Wang, "Modeling and Simulation of Viscoplasticity, Recrystallization, and Softening of Alloyed Steel During Hot Rolling Process," *Missouri University of Science and Technology*, 2018. [Google Scholar] [Publisher Link]

[53] Yonghua Duan et al., "Developed Constitutive Models, Processing Maps and Microstructural Evolution of Pb-Mg-10Al-0.5B Alloy," *Materials Characterization*, vol. 129, pp. 353-366, 2017. [CrossRef] [Google Scholar] [Publisher Link]

[54] Xin Hou et al., "Stress-Strain Curves and Modified Material Constitutive Model for Ti-6Al-4V Over the Wide Ranges of Strain Rate and Temperature," *Materials*, vol. 11, no. 6, pp. 1-13, 2018. [CrossRef] [Google Scholar] [Publisher Link]

[55] Joshua Priest et al., "A Modified Johnson-Cook Constitutive Model for Improved Thermal Softening Prediction of Machining Simulations in C45 Steel," *Procedia CIRP*, vol. 108, pp. 106-111, 2022. [CrossRef] [Google Scholar] [Publisher Link]

[56] Guang Chen et al., "Modeling of Flow Behavior for 7050-T7451 Aluminum Alloy Considering Microstructural Evolution Over a Wide Range of Strain Rates," *Mechanics of Materials*, vol. 95, pp. 146-157, 2016. [CrossRef] [Google Scholar] [Publisher Link]

[57] Y.Q.Li et al., "A New Constitutive Model for Ballistic Roma Plastilina no. 1 Clay," *Mechanics of Advanced Materials and Structures*, vol. 27, no. 24, pp. 2027-2034, 2020. [CrossRef] [Google Scholar] [Publisher Link]

[58] Xinyuan Qian et al., "Dynamic Constitutive Relationship of CuCrZr Alloy based on Johnson-Cook Model," *Nuclear Materials and Energy*, vol. 24, pp. 1-7, 2020. [CrossRef] [Google Scholar] [Publisher Link]

[59] Pierre Tize Mha, Amèvi Tongne, and Olivier Pantalé, "A Generalized Non-Linear Flow Law based on Modified Zerilli-Armstrong Model and its Implementation into Abaqus/Explicit FEM Code," *World Journal of Engineering and Technology*, vol. 10, no. 2, pp. 334-362, 2022. [Google Scholar]

[60] Abdallah Shokry et al., "On the Prediction of the Flow Behavior of Metals and Alloys at a Wide Range of Temperatures and Strain Rates using Johnson–Cook and Modified Johnson–Cook-based Models: A Review," *Materials*, vol. 16, no. 4, pp. 1-53, 2023. [CrossRef] [Google Scholar] [Publisher Link]

[61] Gordon R. Johnson, "A Constitutive Model and Data for Metals Subjected to Large Strains, High Strain Rates and High Temperatures," *Proceedings of the 7th International Symposium on Ballistics*, The Hague, Netherlands, 1983. [Google Scholar] [Publisher Link]

[62] X. Wang et al., "Modeling of Mass Flow Behavior of Hot Rolled Low Alloy Steel based on Combined Johnson-Cook and Zerilli-Armstrong Model," *Journal of Materials Science*, vol. 52, no. 5, pp. 2800-2815, 2017. [CrossRef] [Google Scholar] [Publisher Link]

[63] M. Burley et al., "Johnson-Cook Parameter Evaluation from Ballistic Impact Data via Iterative FEM Modelling," *International Journal of Impact Engineering*, vol. 112, pp. 180-192, 2018. [CrossRef] [Google Scholar] [Publisher Link]

[64] Shucong Xu, Lin Yuan, and Debin Shan, "An Artificial Neural Network Constitutive Model to Predict High Temperature Flow Behaviour in 18Ni (250) Maraging Steel," *Journal of Materials Research and Technology*, vol. 37, pp. 157-172, 2025. [CrossRef] [Google Scholar] [Publisher Link]

[65] Jun Cai, Kuaishe Wang, and Yingying Han, "A Comparative Study on Johnson Cook, Modified Zerilli–Armstrong and Arrhenius-Type Constitutive Models to Predict High-Temperature Flow Behavior of Ti–6Al–4V Alloy in α+ β Phase," *High Temperature Materials and Processes*, vol. 35, no. 3, pp. 297-307, 2016. [CrossRef] [Google Scholar] [Publisher Link]

[66] Abdallah Shokry, and Per Ståhle, "A Methodology for using Kalman Filter to Determine Material Parameters from Uncertain Measurements," *Materials Discovery*, vol. 2, pp. 1-15, 2015. [CrossRef] [Google Scholar] [Publisher Link]

[67] H. Ahmed et al., "An Investigation of the Experimental and Numerical Ballistic Response of 12.7mm AP Tracer Projectile against Al2O3/Al 5083-H116 Bi-Layer Armour," *The International Journal of Multiphysics*, vol. 15, no. 2, pp. 119-138, 2021. [Google Scholar] [Publisher Link]

[68] Eckart Uhlmann et al., "Modelling the Age-related Decrease in Ballistic Limit Velocity of Polycarbonate Vision Panels using a Johnson-Cook Material Model Coupled with Variable Failure Criteria," *Journal of Machine Engineering*, vol. 23, no. 3, pp. 86-97, 2023. [CrossRef] [Google Scholar] [Publisher Link]

[69] P. Ludwik, *Elements of Technological Mechanics*, 1st ed., Springer Berlin, Heidelberg, 1909. [CrossRef] [Google Scholar] [Publisher Link]

[70] Eric Voce, "The Relationship between Stress and Strain for Homogeneous Deformation," *Journal of the Institute of Metals*, vol. 74, pp. 537-562, 1948. [Google Scholar] [Publisher Link]

[71] Sidney Chocron, and Charles E. Anderson Jr "Review and Assessment of Failure Models Applicable to Ballistic Impact Simulations of Ductile Materials," 2010. [Google Scholar]

[72] Hubert W. Meyer Jr, *A Modified Zerilli-Armstrong Constitutive Model Describing the Strength and Localizing Behavior of Ti-6A1-4V*, 2006. [Google Scholar]

[73] Sung-Ju Park et al., "Comparative Study on Various Ductile Fracture Models for Marine Structural Steel EH36," *Journal of Ocean Engineering and Technology*, vol. 33, no. 3, pp. 259-271, 2019. [CrossRef] [Google Scholar] [Publisher Link]

[74] Lingyi Sun et al., "Mechanical Behavior of Material Removal under Various Rake Angle Diamond Tool Ultra-Precision Cutting of Titanium Alloy," *Journal of Materials Research and Technology*, vol. 38, pp. 1302-1312, 2025. [CrossRef] [Google Scholar] [Publisher Link]

[75] Ali Abd El-Aty et al., "Modelling the Flow Behaviour of Al Alloy Sheets at Elevated Temperatures using a Modified Zerilli–Armstrong Model and Phenomenological-based Constitutive Models," *Materials*, vol. 17, no. 7, pp. 1-20, 2024. [CrossRef] [Google Scholar] [Publisher Link]

[76] Bandar Alzahrani et al., "A Modified Johnson Cook Model-based Kalman Filter Method to Determine the Hot Flow Behavior of Sustainable AA6082 Al Alloy," *Materials*, vol. 17, no. 21, pp. 1-20, 2024. [CrossRef] [Google Scholar] [Publisher Link]

[77] Jianli He et al., "A Modified Johnson-Cook Model for 10% Cr Steel at Elevated Temperatures and a Wide Range of Strain Rates," *Materials Science and Engineering: A*, vol. 715, pp. 1-9, 2018. [CrossRef] [Google Scholar] [Publisher Link]

[78] Yanhua Zhao et al., "A Comparative Study on Johnson-Cook and Modified Johnson-Cook Constitutive Material Model to Predict the Dynamic Behavior Laser Additive Manufacturing FeCr Alloy," *Journal of Alloys and Compounds*, vol. 723, pp. 179-187, 2017. [CrossRef] [Google Scholar] [Publisher Link]

[79] Liqun Niu et al., "A Modified Johnson-Cook Model Considering Strain Softening of A356 Alloy," *Materials Science and Engineering: A*, vol. 789, pp. 1-10, 2020. [CrossRef] [Google Scholar] [Publisher Link]

[80] A. Iturbe et al., "Mechanical Characterization and Modelling of Inconel 718 Material Behavior for Machining Process Assessment," *Materials Science and Engineering: A*, vol. 682, pp. 441-453, 2017. [CrossRef] [Google Scholar] [Publisher Link]

[81] Jianjun Wang et al., "Modified Johnson-Cook Description of Wide Temperature and Strain Rate Measurements Made on a Nickel-base Superalloy," *Materials at High Temperatures*, vol. 34, no. 3, pp. 157-165, 2017. [CrossRef] [Google Scholar] [Publisher Link]

[82] Dipti Samantaray et al., "A Thermo-Viscoplastic Constitutive Model to Predict Elevated-Temperature Flow Behaviour in a Titanium-Modified Austenitic Stainless Steel," *Materials Science and Engineering: A*, vol. 526, no. 1-2, pp. 1-6, 2009. [CrossRef] [Google Scholar] [Publisher Link]

[83] W.J. Kang et al., "Modified Johnson-Cook Model for Vehicle Body Crashworthiness Simulation," *International Journal of Vehicle Design*, vol. 21, no. 4-5, pp. 424-435, 2004. [CrossRef] [Google Scholar] [Publisher Link]

[84] Hea Couque, R. Boulanger, and F. Bornet, "A Modified Johnson-Cook Model for Strain Rates Ranging from 10^{-3} to 10^{5} s^{-1}," *Journal de Physique IV (Proceedings)*, vol. 134, pp. 87-93, 2006. [CrossRef] [Google Scholar] [Publisher Link]

[85] G.R. Johnson et al., "Strain-Rate Effects for High-Strain-Rate Computations," *Journal de Physique IV (Proceedings)*, vol. 134, pp. 391-396, 2006. [CrossRef] [Google Scholar] [Publisher Link]

[86] Xiangyu Wang et al., "Dynamic Behavior and a Modified Johnson-Cook Constitutive Model of Inconel 718 at High Strain Rate and Elevated Temperature," *Materials Science and Engineering: A*, vol. 580, pp. 385-390, 2013. [CrossRef] [Google Scholar] [Publisher Link]

[87] Rohan Chakrabarty, and Jun Song, "A Modified Johnson-Cook Material Model with Strain Gradient Plasticity Consideration for Numerical Simulation of Cold Spray Process," *Surface and Coatings Technology*, vol. 397, 2020. [CrossRef] [Google Scholar] [Publisher Link]

[88] M.A. Meyers et al., "High-Strain, High-Strain-Rate Behavior of Tantalum," *Metallurgical and Materials Transactions A*, vol. 26, no. 10, pp. 2493-2501, 1995. [CrossRef] [Google Scholar] [Publisher Link]

[89] Feng Zhang et al., "The Modified Temperature Term on Johnson-Cook Constitutive Model of AZ31 Magnesium Alloy with {0002} Texture," *Journal of Magnesium and Alloys*, vol. 8, no. 1, pp. 172-183, 2020. [CrossRef] [Google Scholar] [Publisher Link]

[90] William K. Rule, and S.E. Jones, "A Revised form for the Johnson-Cook Strength Model," *International Journal of Impact Engineering*, vol. 21, no. 8, pp. 609-624, 1998. [CrossRef] [Google Scholar] [Publisher Link]

[91] Zhi-jun Tao et al., "A Modified Johnson-Cook Model for NC Warm Bending of Large Diameter Thin-Walled Ti-6Al-4V Tube in Wide Ranges of Strain Rates and Temperatures," *Transactions of Nonferrous Metals Society of China*, vol. 28, no. 2, pp. 298-308, 2018. [CrossRef] [Google Scholar] [Publisher Link]

[92] Hyunho Shin, and Jong-Bong Kim, "A Phenomenological Constitutive Equation to Describe Various Flow Stress Behaviors of Materials in Wide Strain Rate and Temperature Regimes," *Journal of Engineering Materials and Technology*, vol. 132, no. 2, 2010. [CrossRef] [Google Scholar] [Publisher Link]

[93] Amit Kumar Maheshwari et al., "Modified Johnson-Cook Material Flow Model for Hot Deformation Processing," *Journal of Materials Science*, vol. 45, no. 4, pp. 859-864, 2010. [CrossRef] [Google Scholar] [Publisher Link]

[94] Y.P. Wang et al., "A Modified Johnson-Cook Model for 30Cr2Ni4MoV Rotor Steel Over a Wide Range of Temperature and Strain Rate," *Journal of Materials Science*, vol. 46, no. 9, pp. 2922-2927, 2011. [CrossRef] [Google Scholar] [Publisher Link]

[95] Y.C. Lin, L.-T. Li, and Y.-Q. Jiang, "A Phenomenological Constitutive Model for Describing Thermo-Viscoplastic Behavior of Al-Zn-Mg-Cu Alloy Under Hot Working Condition," *Experimental Mechanics*, vol. 52, no. 8, pp. 993-1002, 2012. [CrossRef] [Google Scholar] [Publisher Link]

[96] Y.C. Lin et al., "Hot Compressive Deformation Behavior of 7075 Al Alloy Under Elevated Temperature," *Journal of Materials Science*, vol. 47, no. 3, pp. 1306-1318, 2012. [CrossRef] [Google Scholar] [Publisher Link]

[97] Weidong Song et al., "A Modified Johnson-Cook Model for Titanium Matrix Composites Reinforced with Titanium Carbide Particles at Elevated Temperatures," *Materials Science and Engineering: A*, vol. 576, pp. 280-289, 2013. [CrossRef] [Google Scholar] [Publisher Link]

[98] Abdallah Shokry, "A Modified Johnson-Cook Model for Flow Behavior of Alloy 800H at Intermediate Strain Rates and High Temperatures," *Journal of Materials Engineering and Performance*, vol. 26, no. 12, pp. 5723-5730, 2017. [CrossRef] [Google Scholar] [Publisher Link]

[99] O. Lurdos, F. Montheillet, and G. Damamme, "Empirical and Physically based Flow Rules Relevant to High Speed Processing of 304L Steel," *International Journal of Material Forming*, vol. 1, no. S1, pp. 1431-1434, 2008. [CrossRef] [Google Scholar] [Publisher Link]

[100] Weixin Yu et al., "The Dynamic Compressive Behavior and Constitutive Models of a Near α TA23 Titanium Alloy," *Materials Today Communications*, vol. 29, pp. 1-9, 2021. [CrossRef] [Google Scholar] [Publisher Link]

[101] Abdallah Shokry, Samer Gowid, and Ghais Kharmanda, "An Improved Generic Johnson-Cook Model for the Flow Prediction of Different Categories of Alloys at Elevated Temperatures and Dynamic Loading Conditions," *Materials Today Communications*, vol. 27, pp. 1-11, 2021. [CrossRef] [Google Scholar] [Publisher Link]

[102] Alban de Vaucorbeil, and Christopher R. Hutchinson, "A Damage and Failure Implementation for the Simulation of Ductile Solids with Total-Lagrangian Smooth Particle Hydrodynamics," *arXiv preprint*, pp. 1-27, 2019. [CrossRef] [Google Scholar] [Publisher Link]

[103] Frank J. Zerilli, and Ronald W. Armstrong, "Dislocation-Mechanics-based Constitutive Relations for Material Dynamics Calculations," *Journal of Applied Physics*, vol. 61, no. 5, pp. 1816-1825, 1987. [CrossRef] [Google Scholar] [Publisher Link]

[104] Charbel Y. Seif, Ilige S. Hage, and Ramsey F. Hamade, "Incorporating Dual BCC/FCC Zerilli-Armstrong and Blue Brittleness Constitutive Material Models into Oxley's Machining Shear Zone Theory," *Journal of Manufacturing Processes*, vol. 50, pp. 663-675, 2020. [CrossRef] [Google Scholar] [Publisher Link]

[105] Dipti Samantaray et al., "An Overview on Constitutive Modelling to Predict Elevated Temperature Flow Behaviour of Fast Reactor Structural Materials," *Transactions of the Indian Institute of Metals*, vol. 63, no. 6, pp. 823-831, 2010. [CrossRef] [Google Scholar] [Publisher Link]

[106] Jing Zhou et al., "Numerical Simulation and Experimental Investigation of Tailored Hot Stamping of Boron Steel by Partial Heating," *Journal of Materials Research and Technology*, vol. 14, pp. 1347-1365, 2021. [CrossRef] [Google Scholar] [Publisher Link]

[107] Dongxin Niu et al., "Constitutive Modeling of the Flow Stress Behavior for the Hot Deformation of Cu-15Ni-8Sn Alloys," *Frontiers in Materials*, vol. 7, pp. 1-10, 2020. [CrossRef] [Google Scholar] [Publisher Link]

[108] Dipti Samantaray et al., "Flow Behavior and Microstructural Evolution During Hot Deformation of AISI Type 316 L (N) Austenitic Stainless Steel," *Materials Science and Engineering: A*, vol. 528, no. 29-30, pp. 8565-8572, 2011. [CrossRef] [Google Scholar] [Publisher Link]

[109] Fan Li et al., "A Comparative Study on Modified and Optimized Zerilli-Armstrong and Arrhenius-Type Constitutive Models to Predict the Hot Deformation Behavior in 30Si2MnCrMoVE Steel," *Journal of Materials Research and Technology*, vol. 20, pp. 3918-3929, 2022. [CrossRef] [Google Scholar] [Publisher Link]

[110] F.S. Qu et al., "The Research on Vacuum Isothermal Bloom for Powder Metallurgy V-5Cr-5Ti Alloy Guiding by the Constitutive Models and the Error Analysis," *International Journal of Refractory Metals and Hard Materials*, vol. 72, pp. 349-366, 2018. [CrossRef] [Google Scholar] [Publisher Link]

[111] A.L. Gurson, "Continuum Theory of Ductile Rupture by Void Nucleation and Growth: Part I-Yield Criteria and Flow Rules for Porous Ductile Media," *Journal of Engineering Materials and Technology*, vol. 99, no. 1, pp. 2-15, 1977. [CrossRef] [Google Scholar] [Publisher Link]

[112] S. Hao, and W. Brocks, "The Gurson-Tvergaard-Needleman-Model for Rate and Temperature-Dependent Materials with Isotropic and Kinematic Hardening," *Computational Mechanics*, vol. 20, no. 1, pp. 34-40, 2014. [CrossRef] [Google Scholar] [Publisher Link]

[113] D.V. Kubair, K.T. Ramesh, and P.K. Swaminathan, "Effect of Shear-Void-Growth-Softening on Adiabatic Shear-Band-Spacing in Ductile Materials," *Acta Mechanica*, vol. 226, no. 12, pp. 4189-4206, 2015. [CrossRef] [Google Scholar] [Publisher Link]

[114] Luke Peterson et al., "Using an Internal State Variable Model Framework to Investigate the Influence of Microstructure and Mechanical Properties on Ballistic Performance of Steel Alloys," *Metals*, vol. 13, no. 7, pp. 1-28, 2023. [CrossRef] [Google Scholar] [Publisher Link]

[115] Bo Ren, and Shaofan Li, "Modeling and Simulation of Large-Scale Ductile Fracture in Plates and Shells," *International Journal of Solids and Structures*, vol. 49, no. 18, pp. 2373-2393, 2012. [CrossRef] [Google Scholar] [Publisher Link]

[116] Guodong Zhang, and Kapil Khandelwal, "Gurson-Tvergaard-Needleman Model Guided Fracture-Resistant Structural Designs Under Finite Deformations," *International Journal for Numerical Methods in Engineering*, vol. 123, no. 14, pp. 3344-3388, 2022. [CrossRef] [Google Scholar] [Publisher Link]

[117] Xiang Zhu, Liangliang Chu, and Guansuo Dui, "Constitutive Modeling of Porous Shape Memory Alloys using Gurson-Tvergaard-Needleman Model Under Isothermal Conditions," *International Journal of Applied Mechanics*, vol. 12, no. 4, 2020. [CrossRef] [Google Scholar] [Publisher Link]

[118] Xiaoxian Chen, "*Numerical Simulation of Effects of Cladding and Superimposed Hydrostatic Pressure on Fracture in Metals Under Tension*," Dissertations and Thesis, McMaster University, 2009. [Google Scholar] [Publisher Link]

[119] Yi Zhang, Eric Lorentz, and Jacques Besson, "Ductile Damage Modelling with Locking-Free Regularised GTN Model," *International Journal for Numerical Methods in Engineering*, vol. 113, no. 13, pp. 1871-1903, 2018. [CrossRef] [Google Scholar] [Publisher Link]

[120] Zijie Song, Zhiqiang Hu, and Jonas W. Ringsberg, "Critical Void Volume Fraction Identification based on Mesoscopic Damage Model for NVA Shipbuilding Steel," *Journal of Marine Science and Application*, vol. 18, no. 4, pp. 444-456, 2019. [CrossRef] [Google Scholar] [Publisher Link]

[121] Can Wang et al., "Influence of Inclusions on Matrix Deformation and Fracture Behavior based on Gurson-Tvergaard-Needleman Damage Model," *Materials Science and Engineering: A*, vol. 756, pp. 405-416, 2019. [CrossRef] [Google Scholar] [Publisher Link]

[122] K. Nahshon, and John W. Hutchinson, "Modification of the Gurson Model for Shear Failure," *European Journal of Mechanics-A/Solids*, vol. 27, no. 1, pp. 1-17, 2008. [CrossRef] [Google Scholar] [Publisher Link]

[123] Viggo Tvergaard, "Influence of Voids on Shear Band Instabilities Under Plane Strain Conditions," *International Journal of Fracture*, vol. 17, no. 4, pp. 389-407, 1981. [CrossRef] [Google Scholar] [Publisher Link]

[124] Donald R. Lesuer, G. Kay, and M. LeBlanc, "Modeling Large-Strain, High-Rate Deformation in Metals," *Engineering Research, Development and Technology*, vol. 100, 1999. [Google Scholar]

[125] Viggo Tvergaard, and Alan Needleman, "Analysis of the Cup-Cone Fracture in a Round Tensile Bar," *Acta Metallurgica*, vol. 32, no. 1, pp. 157-169, 1984. [CrossRef] [Google Scholar] [Publisher Link]

[126] Mohamed Achouri et al., "Implementation and Validation of a Gurson Damage Model Modified for Shear Loading: Effect of Void Growth Rate and Mesh Size on the Predicted Behavior," *Key Engineering Materials*, vol. 504-506, pp. 691-696, 2012. [CrossRef] [Google Scholar] [Publisher Link]

[127] Vegard Schonberg, and Christian Dalheim Øien, "*Simulations of Impact using the Modified Gurson Model*," Dissertation Master thesis, Norwegian University of Science and Technology, 2012. [Google Scholar] [Publisher Link]

[128] Q. Xue et al., "Constitutive Response of Welded HSLA 100 Steel," *Materials Science and Engineering: A*, vol. 354, no. 1-2, pp. 166-179, 2003. [CrossRef] [Google Scholar] [Publisher Link]

[129] J.H. Lee, and J. Oung, "Yield Functions and Flow Rules for Porous Pressure-Dependent Strain-Hardening Polymeric Materials," *Journal of Applied Mechanics*, vol. 67, no. 2, pp. 288-297, 2000. [CrossRef] [Google Scholar] [Publisher Link]

[130] Wei-Zhi Liao et al., "Heat Flow in the Rifted Continental Margin of the South China Sea Near Taiwan and its Tectonic Implications," *Journal of Asian Earth Sciences*, vol. 92, pp. 233-244, 2014. [CrossRef] [Google Scholar] [Publisher Link]

[131] Muhammad Waqar Nasir, Hocine Chalal, and Farid Abed-Meraim, "Formability Limit Prediction of TRIP780 Steel Sheet using Lode Angle Dependent Gurson-based Models with Thomason Coalescence Criterion and Bifurcation Analysis," *AIP Conference Proceedings*, vol. 2113, no. 1, 2019. [CrossRef] [Google Scholar] [Publisher Link]

[132] Ken Nahshon, and Zhenyu Xue, "A Modified Gurson Model and its Application to Punch-Out Experiments," *Engineering Fracture Mechanics*, vol. 76, no. 8, pp. 997-1009, 2009. [CrossRef] [Google Scholar] [Publisher Link]

[133] Liang Xue, "Constitutive Modeling of Void Shearing Effect in Ductile Fracture of Porous Materials," *Engineering Fracture Mechanics*, vol. 75, no. 11, pp. 3343-3366, 2008. [CrossRef] [Google Scholar] [Publisher Link]

[134] Kim Lau Nielsen, and Viggo Tvergaard, "Effect of a Shear Modified Gurson Model on Damage Development in a FSW Tensile Specimen," *International Journal of Solids and Structures*, vol. 46, no. 3-4, pp. 587-601, 2009. [CrossRef] [Google Scholar] [Publisher Link]

[135] Kim Lau Nielsen, and Viggo Tvergaard, "Ductile Shear Failure or Plug Failure of Spot Welds Modelled by Modified Gurson Model," *Engineering Fracture Mechanics*, vol. 77, no. 7, pp. 1031-1047, 2010. [CrossRef] [Google Scholar] [Publisher Link]

[136] Mihal Gologanu, Jean-Baptiste Leblond, and Gilles Perrin, "A Micromechanically based Gurson-Type Model for Ductile Porous Metals Including Strain Gradient Effects," *ASME International Mechanical Engineering Congress and Exposition*, vol. 17629, pp. 47-56, 1995. [CrossRef] [Google Scholar] [Publisher Link]

[137] Thomas Pardoen, and John W. Hutchinson, "An Extended Model for Void Growth and Coalescence," *Journal of the Mechanics and Physics of Solids*, vol. 48, no. 12, pp. 2467-2512, 2000. [CrossRef] [Google Scholar] [Publisher Link]

[138] J.B. Leblond, G. Perrin, J. Devaux, "An Improved Gurson-Type Model for Hardenable Ductile Metals," *European Journal of Mechanics. A. Solids*, vol. 14, no. 4, pp 499-527, 1995. [Google Scholar] [Publisher Link]

[139] Hadi Bakhshan, Eugenio Oñate, and Josep Maria Carbonell i Puigbó, "A Review of the Constitutive Modelling of Metals and Alloys in Machining Process," *Archives of Computational Methods in Engineering*, vol. 31, no. 3, pp. 1611-1658, 2024. [CrossRef] [Google Scholar] [Publisher Link]

[140] S.R. Chen, G.T.III. Gray, and S.R. Bingert, "*Mechanical Properties and Constitutive Relations for Tantalum and Tantalum Alloys Under High-Rate Deformation*," Los Alamos National Lab, 1996. [Google Scholar] [Publisher Link]

[141] Cheng Chen et al., "A Comparative Study of a Back Propagation Artificial Neural Network and a Zerilli–Armstrong Model for Pure Molybdenum during Hot Deformation," *International Journal of Refractory Metals and Hard Materials*, vol. 25, no. 5-6, pp. 411-416, 2007. [CrossRef] [Google Scholar] [Publisher Link]

[142] Azhari Sastranegara et al., "Finite Element Analysis on Ballistic Impact Performance of Multi-Layered Bulletproof Vest Impacted by 9 Mm Bullet," *Sinergi*, vol. 27, no. 1, pp. 15-22, 2023. [CrossRef] [Google Scholar] [Publisher Link]

[143] Musa Ethem Haksever et al., "Three-Dimensional Ballistic Impact Limit Maps of Glare Composites: An Experimental, Numerical, and Svr-based Machine Learning Investigation," *Numerical, and SVR-based Machine Learning Investigation*, pp. 1-44, 2026. [CrossRef] [Google Scholar] [Publisher Link]

[144] Andrzej Kubit et al., "Three-Dimensional Smooth Particle Hydrodynamics Modeling and Experimental Analysis of the Ballistic Performance of Steel-based FML Targets," *Materials*, vol. 15, no. 10, pp. 1-20, 2022. [CrossRef] [Google Scholar] [Publisher Link]

[145] Laura von Rueden et al., "Combining Machine Learning and Simulation to a Hybrid Modelling Approach: Current and Future Directions," *Advances in Intelligent Data Analysis XVIII, 18th International Symposium on Intelligent Data Analysis*, Konstanz, Germany, pp. 27-29, 2020. [CrossRef] [Google Scholar] [Publisher Link]

[146] Yogeshwaran Velmurugan, and Chandradass Jeyaseelan, "Experimental and Prediction Analysis of High-Velocity Impact Resistance of 3D Printed PLA and Carbon Fiber Reinforced PLA Composites," *Materials Research Express*, vol. 12, no. 3, pp. 1-20, 2025. [CrossRef] [Google Scholar] [Publisher Link]

[147] Sina Ardabili, Amir Mosavi, and Annamária R. Várkonyi-Kóczy, "Advances in Machine Learning Modeling Reviewing Hybrid and Ensemble Methods," *Engineering for Sustainable Future, Selected Papers of the 18th International Conference on Global Research and Education Inter-Academia*, Springer, pp. 215-227, 2020. [CrossRef] [Google Scholar] [Publisher Link]

[148] Phong C.H. Nguyen et al., "Challenges and Opportunities for Machine Learning in Multiscale Computational Modeling," *Journal of Computing and Information Science in Engineering*, vol. 23, no. 6, pp. 1-8, 2023. [CrossRef] [Google Scholar] [Publisher Link]

[149] Hartmut Fischer, "Polymer Nanocomposites: From Fundamental Research to Specific Applications," *Materials Science and Engineering: C*, vol. 23, no. 6-8, pp. 763-772, 2003. [CrossRef] [Google Scholar] [Publisher Link]

[150] Christopher Idumah, "Recent Advancements in Self-Healing Polymers, Polymer Blends, and Nanocomposites," *Polymers and Polymer Composites*, vol. 29, no. 4, pp. 246-258, 2021. [CrossRef] [Google Scholar] [Publisher Link]

[151] Kritika Chaudhary, and Balasubramanian Kandasubramanian, "Self-Healing Nanofibers for Engineering Applications," *Industrial and Engineering Chemistry Research*, vol. 61, no. 11, pp. 3789-3816, 2022. [CrossRef] [Google Scholar] [Publisher Link]

[152] M.R. Kessler, "Self-Healing: A New Paradigm in Materials Design," *Proceedings of the Institution of Mechanical Engineers, Part G: Journal of Aerospace Engineering*, vol. 221, no. 4, pp. 479-495, 2007. [CrossRef] [Google Scholar] [Publisher Link]

[153] Manojit Pusty, and Parasharam M. Shirage, "Insights and Perspectives on Graphene-PVDF based Nanocomposite Materials for Harvesting Mechanical Energy," *Journal of Alloys and Compounds*, vol. 904, pp. 1-32, 2022. [CrossRef] [Google Scholar] [Publisher Link]

[154] Mica Grujicic et al., "A Ballistic Material Model for Cross-Plied Unidirectional Ultra-High Molecular-Weight Polyethylene Fiber-Reinforced Armor-Grade Composites," *Materials Science and Engineering: A*, vol. 498, no. 1-2, pp. 231-241, 2008. [CrossRef] [Google Scholar] [Publisher Link]

[155] I.F. Saruhan, and R. Gunes, "Comparison of the Ballistic Performance of Kevlar and UHMWPE Helmets using FEM," *Defence Science Journal*, vol. 74, no. 6, pp. 867-877, 2024. [CrossRef] [Google Scholar] [Publisher Link]

[156] H. van der Werff, and U. Heisserer, "High-Performance Ballistic Fibers: Ultra-High Molecular Weight Polyethylene (UHMWPE)," *Advanced Fibrous Composite Materials for Ballistic Protection*, pp. 71-107, 2016. [CrossRef] [Google Scholar] [Publisher Link]

[157] David J. Krzypow, and Clare M Rimnac, "Cyclic Steady State Stress-Strain Behavior of UHMW Polyethylene," *Biomaterials*, vol. 21, no. 20, pp. 2081-2087, 2000. [CrossRef] [Google Scholar] [Publisher Link]

[158] K.R. Dinesh, and Gururaj Hatti, "Tribological and Mechanical Properties of UHMWPE Polymer Composite Filled with Tio2 and Al2O3 Particles used as TKR Implant," *International Journal of Innovative Technology and Exploring Engineering*, vol. 9, no. 6, pp. 991-995, 2020. [CrossRef] [Google Scholar] [Publisher Link]

[159] Amanda L. Forster et al., "Long-Term Stability of UHMWPE Fibers," *Polymer Degradation and Stability*, vol. 114, pp. 45-51, 2015. [CrossRef] [Google Scholar] [Publisher Link]